Preliminary Studies on the Effects of Glycosyl Triazoles on C2C12 Stem Cells

by

Traci M. Clymer

Submitted in Partial Fulfillment of the Requirements

For the Degree of

Masters of Science in the

Chemistry Program

YOUNGSTOWN STATE UNIVERSITY

August, 2010

Traci M. Clymer

I hereby release this thesis to the public. I understand this thesis will be made available from the OhioLINK Center and the Maag Library Circulation Desk for public access. I also authorize the University or other individuals to make copies of this dissertation as needed for scholarly research.

Signature:

_____

Traci M. Clymer Date

Approvals:

_____

Dr. Peter Norris Date

Thesis Advisor

_____

Dr. Gary Walker Date

Committee Member

_____

Dr. Nina Stourman Date

Committee Member

_____

Dr. Peter J. Kasvinsky Date

Dean of Graduate Studies and Research

Abstract

The C2C12 line of cells differentiates rapidly to form contractile myotubes which give rise to contractile skeletal muscle. The muscle fibers formed from these cells contain a high concentration of glycogen and are heavily reliant on glycolytic enzymes. 1,2,3-triazoles have been shown to have a wide array of biological activities and may mimic peptide bonds or phosphate groups. For this reason it is proposed that glycosyl triazoles may have some effect on the development or function of C2C12 cells as they differentiate.

Acknowledgements

I would like to thank the Youngstown State University Department of Chemistry and the School of Graduate Studies for allowing me the opportunity to pursue the Master of Science degree. I would also like to thank Dr. Gary Walker and the Department of Biology for allowing me the opportunity and guidance to work on a very unique and collaborative project. I would like to thank Dr. Stourman for her guidance as a committee member, and Dr. John Jackson for providing me with a great deal of the knowledge and skills necessary to complete this work. I would also like to thank Dr. Tim Wagner for his encouragement and advice throughout my time at YSU.

I would especially like to thank Dr. Peter Norris for his help and guidance as an advisor and for arranging such an interesting project for me to work on which has allowed me to gain exposure to different areas of research which I'm sure will help me in my future career.

I would like to thank all of my fellow students working in both the Norris and Walker labs and my graduate classmates. I would especially like to thank Antony and John for keeping me entertained during those long days in lab and Kyle for pushing me and supporting me no matter how much I whined and complained.

Last but not least I would like to thank my family and friends for their love and support throughout the years.

Table of Contents

Title Page…….....i

Signature Page…….ii

Abstract……...iii

Acknowledgments……..iv

Table of Contents…….v

List of Schemes……...vi

List of Equations……..…vi

List of Figures…….....vi

Introduction……...1

Statement of Problem……..13

Results and Discussion……14

Conclusion……...…28

Future Work…….29

Experimental……30

References……45

Appendix A……..48

Appendix B……...64

List of Schemes

Scheme 1. Synthesis of D-glucosyl azide (**3**)…….15

Scheme 2. Proposed mechanism of copper catalyst……...17

Scheme 3. Synthesis of dimethyl (diazomethyl)phosphonate (**11**)……21

List of Equations

Equation 1. Synthesis of triazole alcohol (**4**)……...18

Equation 2. Synthesis of aldehyde (**5**) from alcohol (**4**)……..19

Equation 3. Synthesis of *p*-acetamidobenzenesulfonyl azide (**9**)……20

Equation 4. Synthesis of alkyne (**6**) from aldehyde (**5**) with (**11**) as a reagent...22

Equation 5. Synthesis of triazole (**7**) from azide (**3**)……...22

Equation 6. Deprotection of azide (**3**) to yield (**13**)……23

Equation 7. Deprotection of triazole (**4**) to yield (**14**)……23

Equation 8. Deprotection of triazole (**7**) to yield (**15**)……24

Equation 9. Deprotection of dodecyne-derived triazole (**12**) to yield (**16**)…….24

List of Figures

Figure 1. Binding of myosin to actin in myofibrils……...2

Figure 2. Structure of D-glucose……3

Figure 3. Interconversion of α and β anomers of D-glucose…….4

Figure 4. Chair conformations of β-D-glucopyranose……...5

Figure 5. Inhibitors of glycogen phosphorylase……8

Figure 6. Vineomycinone B2……9

Figure 7. Digoxin……..9

Figure 8. Erythromycin A, Streptomycin, and Daunomycin……..10

Figure 9. Ara-C, Acyclovir, and AZT……11

Figure 10. Gauche (left) and anti-periplanar (right) conformations of (**2**) and (**3**) Respectively……16

Figure 11. X-ray structure of deprotected triazole (**16**)…….24

Figure 12. Packing view of triazole (**16**)……...25

Figure 13. Control C2C12 muscle cells……26

Figure 14. Treated C2C12 cells……27

Figure 15. SDS-PAGE gel……....28

Figure 16. 400 MHz ^{1}H spectrum of glucosyl bromide (**2**)……..49

Figure 17. 400 MHz ^{1}H spectrum of glucosyl azide (**3**)……...50

Figure 18. 400 MHz ^{1}H spectrum of glucosyl triazole (**4**)…….51

Figure 19. 400 MHz ^{1}H spectrum of glucosyl triazole (**5**)……..…52

Figure 20. 400 MHz ^{1}H spectrum of glucosyl triazole (**6**)……..…53

Figure 21. Mass spectrum of glucosyl triazole (**6**)…….54

Figure 22. 400 MHz ^{1}H spectrum of glucosyl triazole (**7**)…….55

Figure 23. 400MHz ^{1}H spectrum of *p*-acetamidobenzenesulfonyl azide (**9**)….56

Figure 24. 100 MHz ^{13}C spectrum of *p*-acetamidobenzenesulfonyl azide (**9**)..57

Figure 25. 400 MHz ^{1}H spectrum of dimethyl (diazomethyl)phosphonate (**11**)

……..58

Figure 26. 161 MHz ^{31}P spectrum of dimethyl (diazomethyl)phosphonate (**11**)

……..59

Figure 27. 400 MHz ^{1}H spectrum of deprotected glucosyl azide (**13**)……...60

Figure 28. 400 MHz ^{1}H spectrum of deprotected glucosyl triazole (**14**)……...61

Figure 29. 400 MHz ^{1}H spectrum of deprotected glucosyl triazole (**15**)……...62

Figure 30. 400 MHz ^{1}H spectrum of deprotected glucosyl triazole (**16**)……...63

Figure 31. X-ray crystal structure of glucosyl triazole (**16**)……...64

Introduction

Myoblasts

Skeletal myogenesis is the process by which myoblasts fuse together to ultimately form skeletal muscle. It is very precise and involves very specific changes in cell morphology and the arrangement of cells into tissue.[1] Myoblasts, which arise from mesodermal mesenchymal cells, are the stem cells from which muscle tissue is eventually formed. They are fairly nonspecific which allows for easy manipulation making them a good choice for cell culture. Myoblasts have a central nucleus and are somewhat elongated in shape. They are similar in structure to any other undifferentiated cells in that they have a lot of free ribosomes, which is typical of cells that synthesize proteins for endogenous use, and very little membranous specializations. In myoblasts the synthesized proteins myosin and actin are polymerized as filamentous structures which are specifically oriented to one another giving rise to myofibrils (Figure 1).[2] Both myosin and actin are contractile proteins and give muscle the ability to contract. Overlapping units of myosin make up thick filaments and thin filaments are composed actin. Each actin of the thin filament possesses a binding site for the myosin head of the thick filament. The temporary binding of these two filaments causes muscle movement.[3,4]

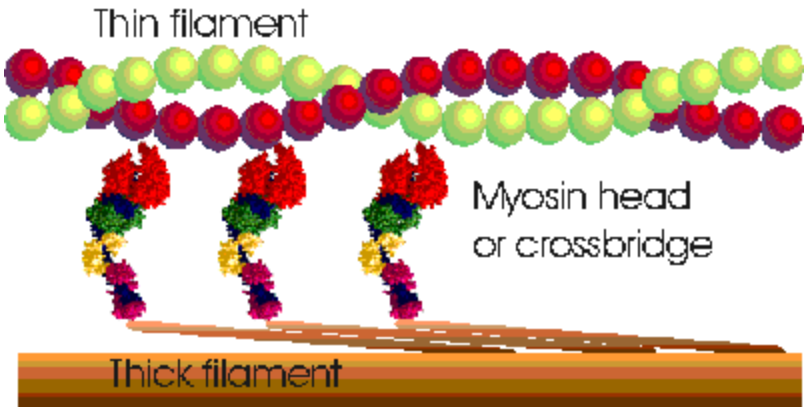

Figure 1: Binding of mysoin to actin in myofibrils.[3]

It is well established that myogenesis is controlled by a repression-type growth factor-dependant mechanism. This means that the process is inhibited by specific growth factors like fibroblast growth factor (FGF) and transforming growth factor type-β (TGF-β) or mitogens present in the serum that block the expression of muscle-specific genes which stimulate differentiation and eventual formation of muscle fibers. Thus differentiation is triggered by the depletion of these growth factors below a critical level.[5,6,7]

It was originally believed that the determination of muscle cells was controlled by a single myogenic master gene, MyoD. It is now known that determination of the muscle phenotype is regulated by a whole family of myogenic factors, which include MyoD, myogenin, myf-5, and MRF4.[8] These factors are confined to the nucleus and only expressed in skeletal muscle. Although only found naturally in skeletal muscle cells these factors may activate myogenesis when transfected into many other types of mesodermal cells.[9] These factors act in a sequential manner and are over 80% homologous in structure within the 70 amino acid segment which contains the region responsible for DNA binding and a helix-loop-helix (HLH) motif that

mediates dimerization. HLH proteins like these bind to the DNA consensus sequence CANNTG which is also known as an E-box.[10]

Carbohydrates

Carbohydrates are mostly composed of atoms of carbon, hydrogen and oxygen. The simplest form of carbohydrate is a monosaccharide, or "simple" sugar. They can best be described as aldehyde or ketone derivatives of straight-chain polyhydroxyl alcohols and must contain at least three carbon atoms. Monosaccharides are further divided into aldoses and ketoses; those with aldehyde groups are aldoses and those with ketone groups are ketoses. In addition, monosaccharides with three carbon atoms may be referred to as trioses, those with four as tetroses and so on.

One common example of a monosaccharide is D-glucose (Figure 2):

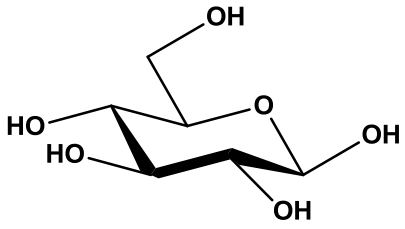

Figure 2: Structure of D-glucose.

D-Glucose interconverts between the cyclic form shown above and the linear form. When the linear form cyclizes the carbon of the carbonyl group, which is also referred to as the anomeric carbon, will become a chiral center capable of two configurations. These two stereoisomers are called anomers since they differ in configuration at the anomeric carbon. In the α anomer the OH substituent of the anomeric carbon is opposite the CH_2OH substituent of

the chiral carbon which determines whether the sugar has a D or L configuration. In the β anomer the OH group is on the same side as the CH_2OH group. In aqueous solution these two anomers readily interconvert meaning that at equilibrium D-glucose is a mixture of the two anomers with about 60 % in the β configuration, about 35 % in the α, and a very small amount in the open chain linear form (Figure 3).

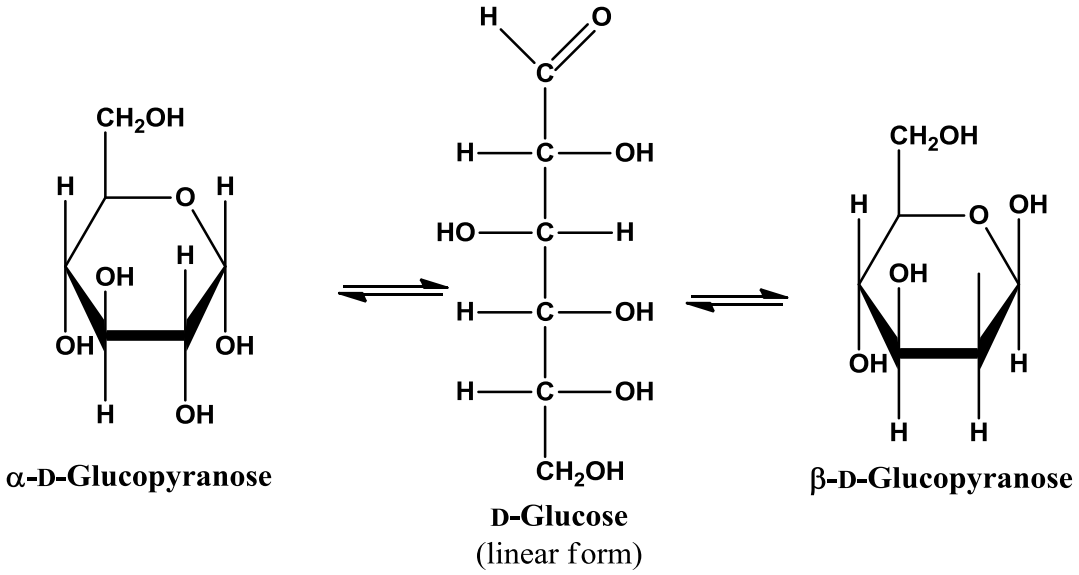

Figure 3: Interconversion of α and β anomers of D-glucose.

The 6-membered ring formed by a sugar is referred to as a pyranose and a five-membered ring is called a furanose. Pyranose rings adopt chair conformations in the same manner as cyclohexane. This means there are two possible main chair conformations for each anomer of D-glucose. Of course the conformation in which the largest substituents are in equatorial positions will be favored over the more crowded, higher energy axial positions. In the diagram below of β-D-glucopyranose the conformation to the left would be greatly favored. As can be seen in

Figure 4, this conformation has all of the bulky groups in the equatorial position making it very stable.

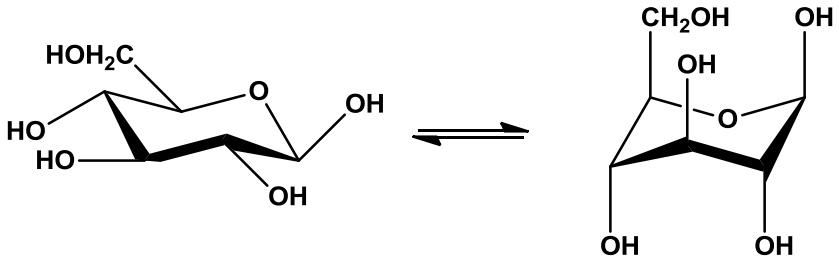

Figure 4: Chair conformations of β-D-glucopyranose.

The anomeric carbon of a sugar can condense with an alcohol through a dehydration reaction in which the sugar loses the anomeric hydroxyl group, while the alcohol loses a proton to release a molecule of water. This process forms what is called a glycosidic bond or linkage between the sugar and the alcohol.[12] The sugars involved in these reactions are also referred to as glycosyl donors and the alcohols as glycosyl acceptors.[13] The products formed in these reactions are called glycosides. There are four different common types of glycosides that can be formed depending on the functionality of the linkage formed. Glycosides formed with *–CR*, *-OR*, *-SR*, and *–NR* linkages are called *C*-glycosides, *O*-glycosides, *S*-glycosides, and *N*-glycosides, respectively.[14]

Mutiple monosaccharides may be linked to one another through glycosidic bonds. These structures are called polysaccharides or *glycans*. They can be further classified as heteropolysaccharides if they contain more than one type of monosaccharide or homopolysaccharides if they do not. Because glycosidic bonds can be formed at any of the hydroxyl groups of a monosaccharide they can form both branched and linear chains unlike proteins or nucleic acids. Dissacharides are the simpliest type of polysaccharide and consist of

just two monosaccharides bound together. Two of the most notable disaccharides are probably lactose, which is found in milk, and sucrose which is more commonly known as table sugar. The most prevelant polysaccharide on earth is cellulose which is a linear polymer composed of several thousand repeating units of glucose linked through glycosidic bonds. Cellulose forms an extensive network of hydrogen bonds which provides strength and rigidity to plant cell walls. Similar to cellulose is chitin which is also very abundant as it is the major component of the exoskeleton in many invertebrates. The only structural difference between the two is that the hydroxyl group of the C2 carbon in the glucose molecules of cellulose is replaced with an acetamido group. Starch, like cellulose is found abundantly in plants, but it serves a very different function. It provides an energy reserve and is stored in the chloroplasts in the form of insoluble granules. These granules are composed of two polymers, α-amylose and amylopectin. α-Amylose consists of thousands of glucose molecules linked together through α-glycosydic bonds in a linear chain. Amylopectin is similar to α-amylose but it is not linear and contains branch points at approximately every 24-30 residues. In animals, energy is stored as the polysaccharide, glycogen. Glycogen is found in all cells but is most concentrated in skeletal muscle and the liver.[12] It is very similar in structure to amylopectin but it is more highly branched with branch points every 8 to 14 residues. This highly branched structure makes glucose more rapidly accessible in instances of metabolic need.[12, 15]

Carbohydrates or polysaccharides can also be found bound to other types of biomolecules. These structures are called glycoconjugates. When carbohydrates are joined by glycosidic linkage with proteins they are termed glycoproteins. If a structure is majorly composed of polysaccharide it is called a proteoglycan.[13]

Glycogen Phosphorylase

The breakdown of glycogen into free units of glucose is called glycogenolysis. It is a three-step process catalyzed by the enzymes glycogen phosphorylase, glycogen debranching enzyme, and phosphoglucomutase. Glycogen phosphorylase catalyzes the rate-controlling step in glycogenolysis and is regulated by both covalent modification and allosteric interactions. The enzyme exists in two forms called phosphorylase *a* and phosphorylase *b*. Phosphorylase *a*, or the phosphorylated form, has a phosphoryl group esterfied to Ser 14. Phosphorylase *b* is the un-phosphorylated form. Adenosine triphosphate (ATP), glucose-6-phosphate (G6P), and glucose are allosteric inhibitors of phosphorylase and adenosine monophosphate (AMP) is an allosteric activator. Each of these molecules interact differently with each of the two forms of phosphorylase making the regulation process highly sensitive.[16]

The inhibition of hepatic glycogen phosphorylase is attractive because it could be useful as a potential treatment for type 2 diabetes. This is because the high blood glucose concentration characteristic of this type of diabetes is due, partially, to abnormal production of glucose by the liver. Since glucose phosphorylase catalyzes the first and rate-determining step in the breakdown of glycogen its inhibition may prevent free glucose units from being released.[17] Several glucose-derived amides have shown moderate inhibitory effects against glycogen phosphorylase *b* isolated from rabbit muscle.[18] Triazoles have been shown to mimic the electronic properties of amide bonds which are key to the inhibition of this enzyme.[18]

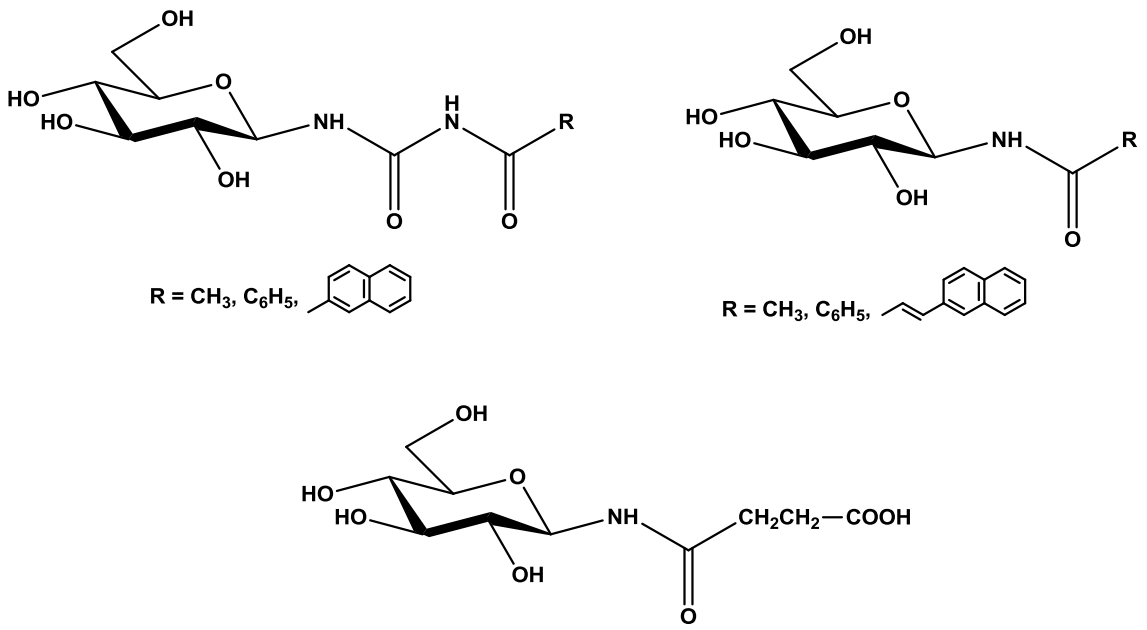

Figure 5: Moderate inhibitors of glycogen phosphorylase *b*.[18]

Glycosides

Many examples of *C*-glycosides have been isolated from microbial and plant sources. *C*-glycosides are important because they are not susceptible to acid- or enzyme-catalyzed hydrolysis meaning they will maintain their structure in the body. They have also been shown to have important pharmacological and biological activity. One example, whose structure is shown below (Figure 6), is vineomycinone B2 which belongs to the vineomycins class of antitumor antibiotics.[15]

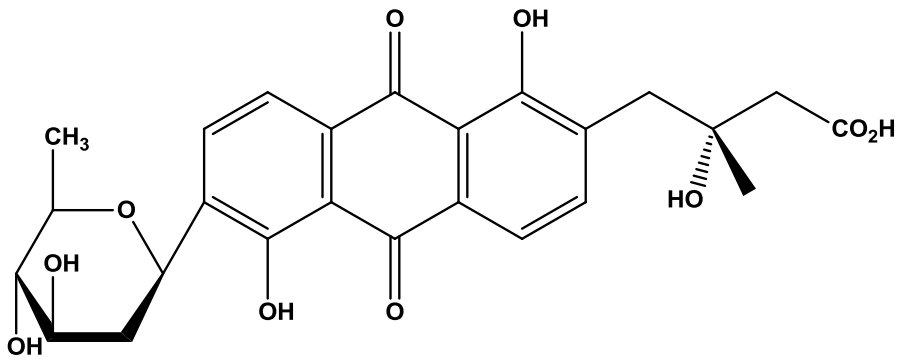

Figure 6: Vineomycinone B2.[15]

O-Glycosides have been isolated from plant, animal, and microbial sources. One important group of *O*-glycosides that are found in plants is the cardiac glycosides. These complex molecules belong to *Digitalis* family which has been named for their digitalis-like effect on the heart. An example of one of these compounds is the popular drug digoxin which is extracted from the foxglove plant.[15]

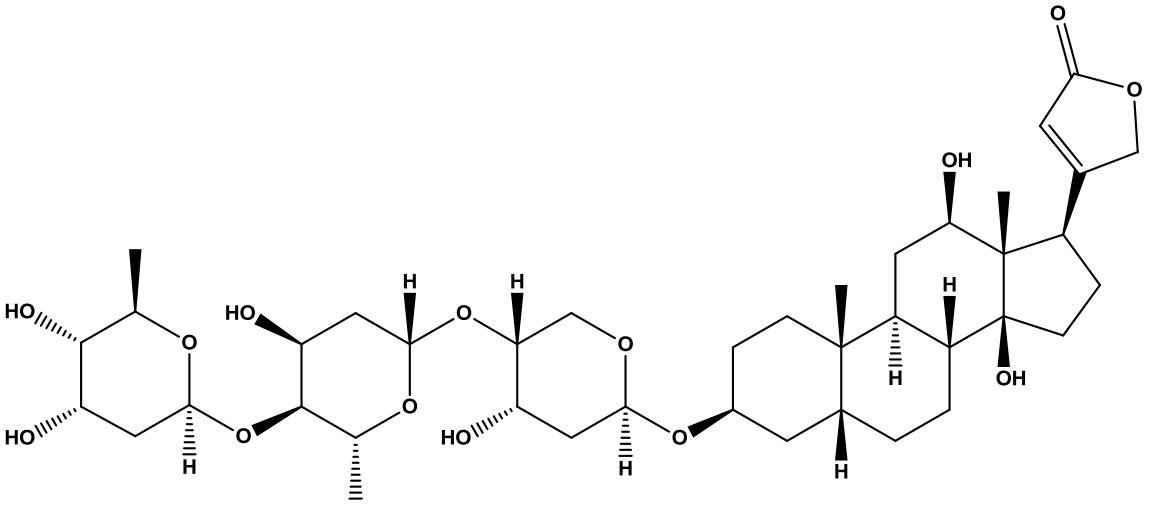

Figure 7: Chemical structure of digoxin.[15]

The presence of *O*-glycosides is very important for animals. They have a major role in detoxification processes through conjugation of foreign and endogenous substances so that they

can be excreted through normal metabolic processes. Finally the *O*-glycosides which have been isolated from microbial sources may be some of the most important due to their antibiotic activity. One interesting characteristic of these glycoside antibiotics is their diversity and distinctiveness in structure. Many of them possess unusual configurations consisting of branched-chain, diamino, alkylamino, and other varied functional groups which are not found in other sources. To illustrate the diversity of these antibiotics, the drugs erythromycin A, streptomycin, and daunomycin are highlighted in Figure 8. Each of these drugs belongs to different classes and has very different structures.[15]

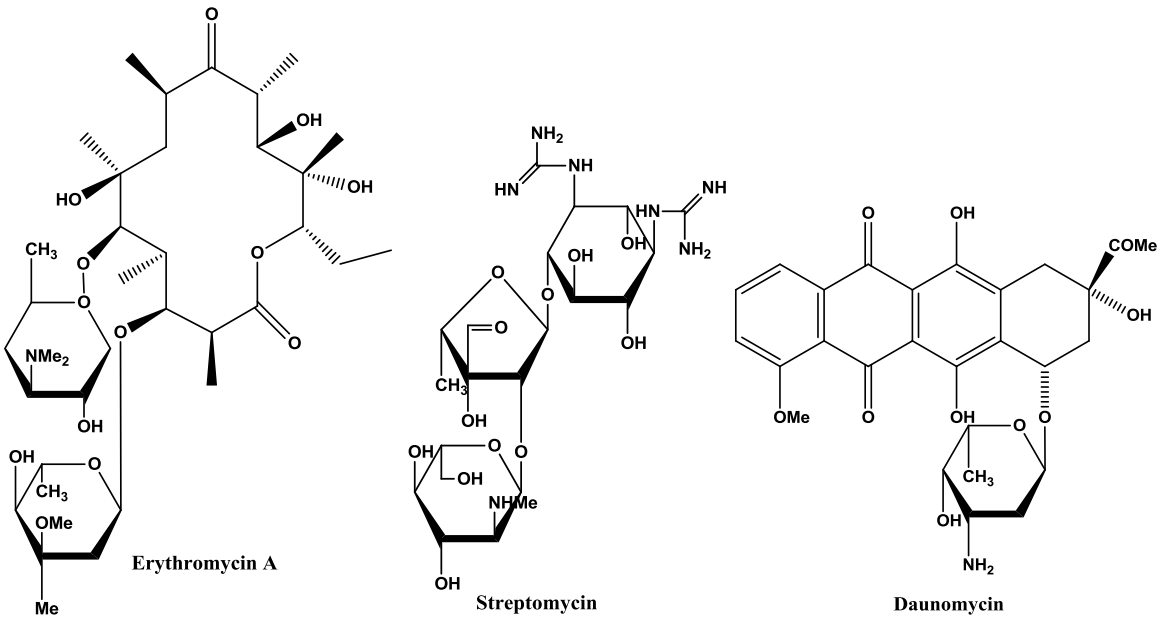

Figure 8: Structures of three *O*-glycoside antibiotics.[15]

Erythromycin A is classified as a macrolide because of its macrocylic lactone and its ability to inhibit protein synthesis at the ribosomal level. It is generally used as a substitute for those who are allergic to penicillin. Streptomycin is part of the aminoglycoside family and also works by interfering with protein biosynthesis by binding to the ribosomes in bacteria. It is most

commonly used as a treatment for tuberculosis. Daunomycin is an anthracycline, which have anti-Gram-positive activity but are not used to treat infections because of their high toxicity to humans. They are, however; used as chemotherapeutic agents because they interculate, or are reversibly included into strands of DNA such that RNA synthesis is inhibited.[15]

N-Glycosides or glycosylamines have many important functions in both biochemistry and biology. Nucleosides are one type of *N*-glycoside that are extremely important in nature and are also as pharmaceuticals. This is because they represent key components of nucleotides and nucleic acids. Compounds belonging to this group have shown a wide array of pharmaceutical activities. Below are three examples (Figure 9), Ara-C which exhibits activity against myelocytic leukemia, Acyclovir, an antiviral agent, and AZT which is a potent antiretroviral used for the treatment of HIV and AIDS.[15]

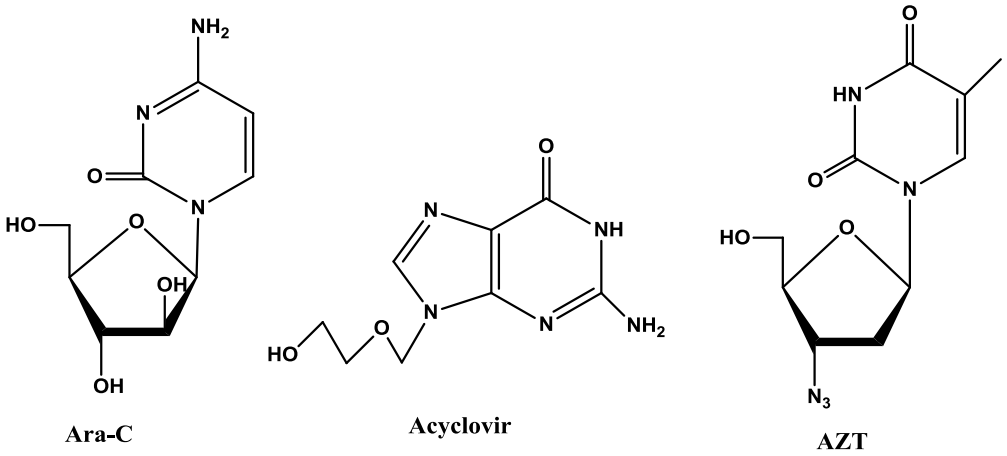

Figure 9: Structures of three *N*-glycoside pharmaceuticals.[15]

N-Glycosyl 1,2,3-Triazoles

N-Glycosyl 1,2,3-triazoles are very stable molecules which are not susceptible to metabolic processes. For this reason they can be useful linkers in the development of biologically active molecules especially those used in drug development. Triazoles have been shown to possess a wide range of biological activities and some have even exhibited inhibition towards β-lactamases.

1,2,3-triazoles can be easily produced through "click" reactions. A reaction may be termed a "click" reaction if it is broad in scope, is simple to perform, gives high yields, uses easily accessible reagents, is unaffected by oxygen or water, and can be easily purified and isolated. Reactions like these are typically used to quickly develop libraries of similar compounds to be used as building blocks in drug design.[14]

Statement of the Problem

The goal of this research was to synthesize glycosyl 1,2,3-triazole derivatives and test their effects on the C2C12 line of stem cells. C2C12 stem cells are myoblasts isolated from mice which give rise to contractile skeletal muscle. Skeletal muscle contains a high concentration of glycogen and is heavily reliant on glycolytic enzymes. Glycosyl 1,2,3-triazoles may have the potential to inhibit the enzyme glycogen phosphorylase which catalyzes the rate-controlling step in the breakdown of glycogen into free units of glucose. Inhibition of this enzyme could have potential as a new treatment for type 2 diabetes.

Results and Discussion

The primary focus of this research was to synthesize glycosyl 1,2,3-triazoles that may possess biological/inhibitory functions which would be useful in drug design and to design a procedure to test their effects on the development of skeletal muscle. There was also a focus on using starting materials that were abundant and cheap. For this reason 1,2,3,4,6-penta-*O*-acetyl-*β*-D-glucose was used to synthesize a glucosyl azide from which most of the other products were derived.

1,2,3-Triazole Synthesis

In the first step 1,2,3,4,6-penta-*O*-acetylated-*β*-D-glucose (**1**, Scheme 1) was treated with 33% hydrobromic acid in acetic acid to produce glucosyl bromide **2** through the S_N1 pathway. The alpha-anomer is preferentially formed due to the anomeric effect which occurs because the anomeric substituent is electronegative. When in the equatorial position the dipoles of the oxygen atom and the adjacent bromine atom are partially aligned causing them to repel but in the axial position the dipoles are opposing making it a lower and more stable energy state. After about 3.5 hours TLC for this reaction showed a new spot burning at a higher R_f value than the starting materials. ^{1}H NMR also indicated formation of the product through the appearance of a doublet at 6.62 ppm and the disappearance of the doublet present at 5.70 ppm in the starting material. These signals correspond to H-1 or the proton attached to the anomeric carbon. The signal is shifted further downfield for the product because the proton experiences more deshielding from the more electronegative bromine atom in the product than from the acetyl group present on the starting material.

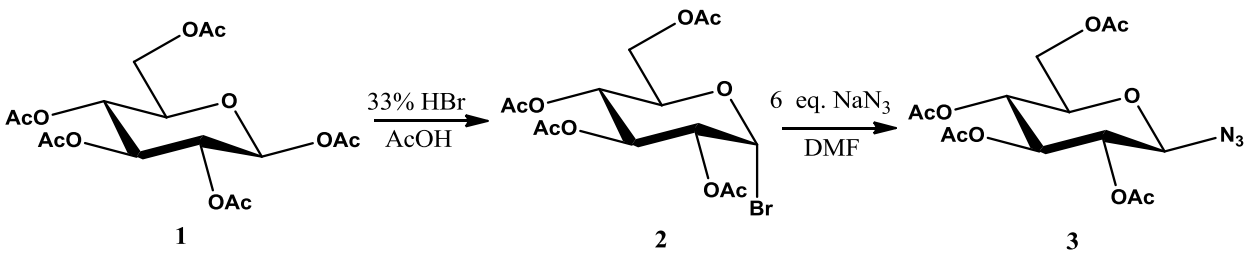

Scheme 1: Synthesis of D-glucosyl azide.

The bromine was added in order to establish a good leaving group that is utilized in the next reaction to produce *β*-glucosyl azide **3**. The crude glucosyl bromide **2** was immediately dissolved in DMF and sodium azide was added and the mixture was left to stir overnight until completion. This reaction proceeds through a stereospecific, S_N2 pathway in which the bromine group in the axial position at the anomeric carbon is replaced by an azide group that ends up in the equatorial position. Completion of this reaction was detected by the appearance of a new spot on the TLC plate burning at a lower R_f value than that of the glucosyl bromide. This procedure produced the glucosyl azide **3** with a 98 % yield. Further evidence of the production of the azide can be seen from ^{1}H NMR which showed a shift upfield of the anomeric proton from 6.62 ppm to 4.64 ppm. The signal is shifted upfield because the azido group provides some shielding of the proton whereas the bromine group deshielded it pushing it downfield. There is also a significant change in the coupling constant for the signal from the anomeric proton. It more than doubles in the azide, increasing from 4.06 Hz to 8.76 Hz. The reason for this increase is the difference in position of the protons at C-1 and C-2. In the glucosyl bromide **2** they are 60 ˚ apart or *gauche* to each other, but in the glucosyl azide **3** they are a full 180˚ apart making them *antiperiplanar* and increasing their coupling constant (Figure 10).

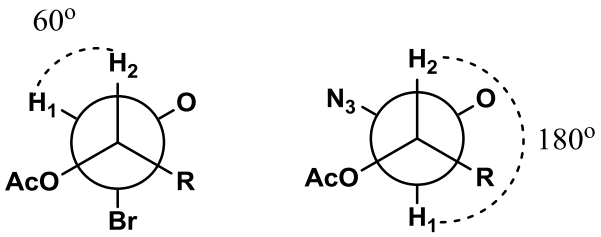

Figure 10: *Gauche* and *antiperiplanar* Newman projections of **2** and **3** respectively.

From glucosyl azide **3** various 1,2,3-triazoles can be formed through cycloaddition reactions with alkynes. This method is a copper(I)-catalyzed adaptation of the classic Huisgen 1,3-dipolar cycloaddition that was discovered concurrently but independently by the Sharpless and Meldal groups in which the addition of a copper(I) catalyst dramatically increases reaction time, eliminates the need for high temperatures, improves regioselectivity to give only the 1,4-regioisomer, and allows for a broader scope of reactants. Below (Scheme 2) is the mechanism proposed by researchers at The Scripps Institute in La Jolla, California for the catalytic cycle. The mechanism was proposed based on calculations and kinetic studies in an effort to explain all the advantages gained with the addition of the copper (I) catalyst. This mechanism produces only the 1,4-regioisomer due to the formation of the Cu-acetylide and its interaction with the electron-rich N-1 of the azide.[19]

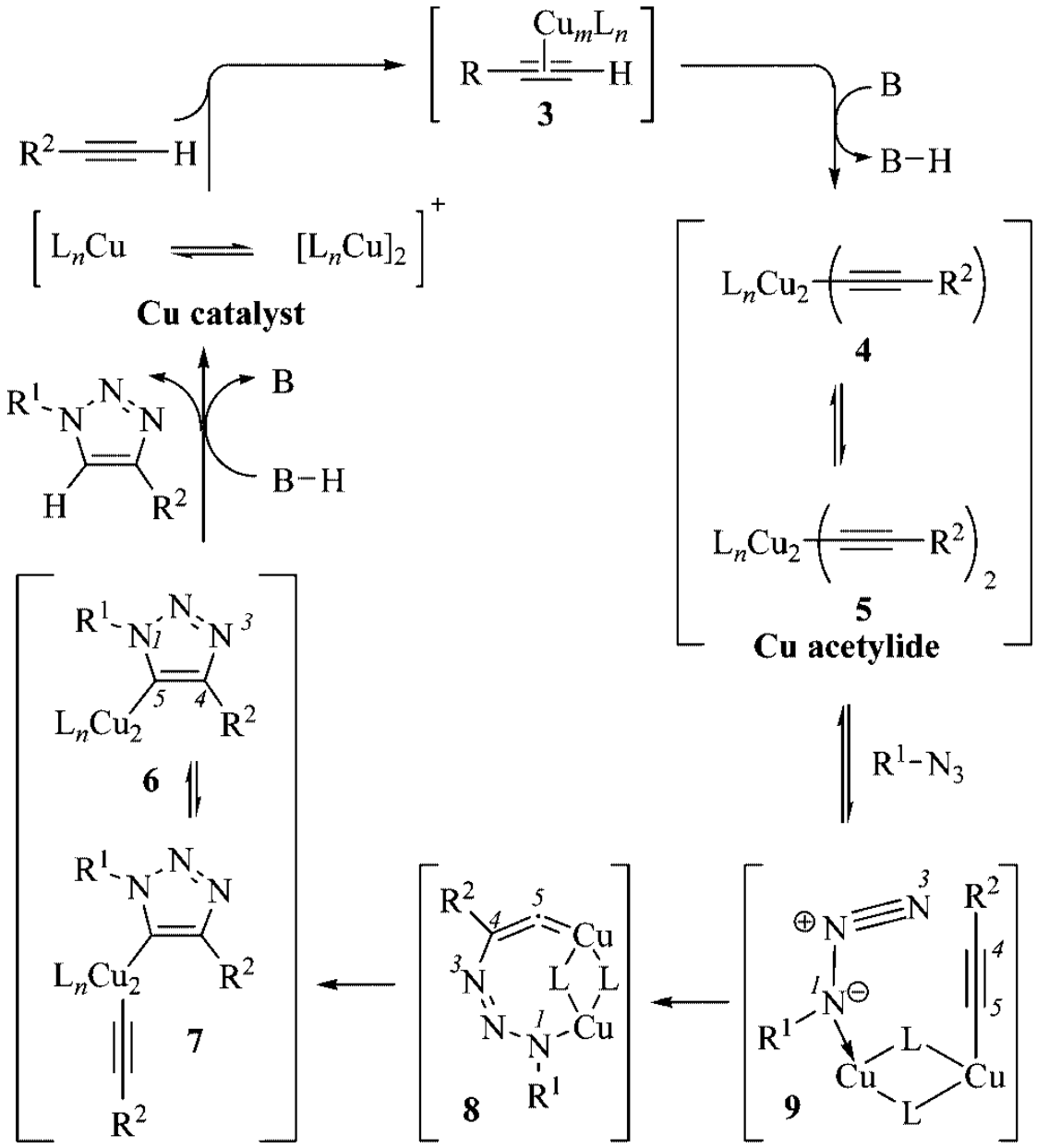

Scheme 2: Proposed mechanism of copper(I) catalysis.[19]

This improved method was utilized in the next reaction to produce glucosyl triazole alcohol **4** from glucosyl azide **3**, propargyl alcohol, copper (II) sulfate, L-ascorbic acid, in 1:1 ethanol/water as solvent. The mixture was allowed to react overnight and then heated under

reflux for 1 hour to drive the reaction to completion which was confirmed by TLC. Since the triazole **4** produced is not soluble in water the ethanol was removed *in vacuo* and the product was precipitated as clear crystals. The crystals were then washed with cold water to remove any remaining copper salts and ^{1}HNMR spectra showed that no further purification was necessary. ^{1}HNMR spectra again showed formation of the product by a shift in the signal of the anomeric proton downfield from 4.64 to 5.86 ppm as well as the introduction of two singlets at 4.82 and 7.79 ppm corresponding to the CH_2 triazole substituent and the triazole H-5 proton, respectively.

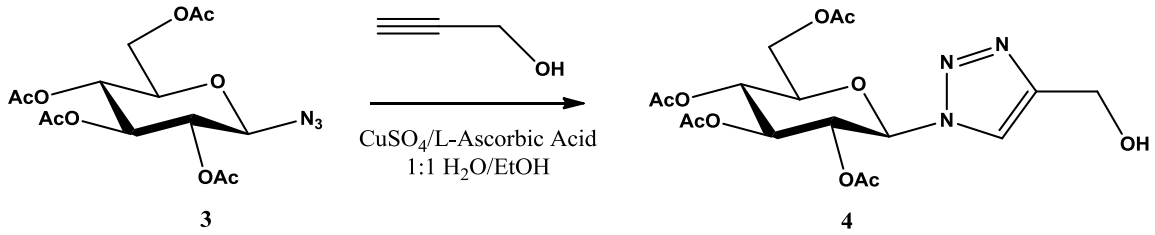

Equation 1: Synthesis of triazole alcohol **4**.

The next reaction was the oxidation of the alcohol **4** to aldehyde **5** (Equation 2). The alcohol **4** was added to 6 equivalents of pyridinium chlorochromate (PCC) and 6 equivalents of 4 Å molecular sieves in methylene chloride and left to stir for 48 hrs until TLC showed consumption of the starting material and a new spot at a higher R_f value. The formation of the aldehyde **5** could also be seen from the appearance of a singlet at 10.15 ppm corresponding to the aldehyde proton. The signal is shifted slightly further downfield than the typical range between 9-10 ppm for aldehydes because the triazole is a weak electron-withdrawing group (EWG). The signal for the triazole proton also shifts further downfield from 7.79 to 8.35 ppm because the aldehyde substituent is a stronger EWG than the alcohol.

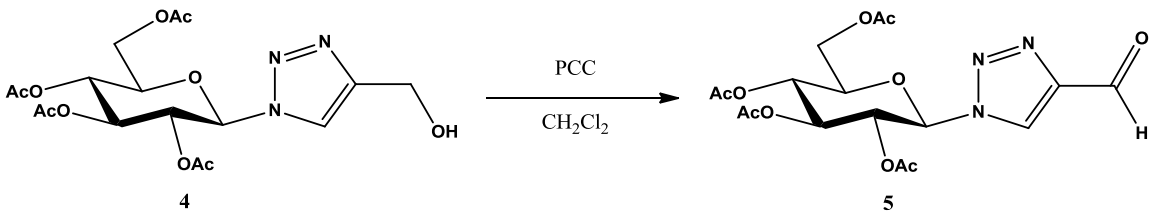

4 5

Equation 2: Synthesis of aldehyde **5** from alcohol **4**.

p-Acetamidobenzenesulfonyl azide (*p*-ABSA, **9**) was synthesized (Equation 3) from *N*-acetyl sulfanilyl chloride (**8**) to be used in the production of dimethyl (diazomethyl)-phosphonate (**11**, Scheme 3) which was in turn was used in attempts to prepare alkyne **6** (Equation 4). Although this reagent (**11**) is readily available, it was reported by Brown *et al.*[17] that their method for the synthesis of dimethyl (diazomethyl)phosphonate gave more consistent yields in a range of 45-50 % when prepared with homemade *p*-ABSA as opposed to commercially available which gave a range from 20-50 %. The procedure used to produce *p*-ABSA (**9**) is a simple one and it produced the product in high yields (78-87%) from very inexpensive materials. A similar reaction takes place as that used to convert the glucosyl bromide **2** to glucosyl azide **3**. Sodium azide was dissolved in acetone and cooled to 0 ˚C, *N*-acetylsulfanilyl chloride was added slowly over 5 minutes and the reaction was warmed to room temperature and left to stir under nitrogen for 2 days. TLC was not especially useful to confirm the completion of this reaction because the R*f* values of the starting material and the product were almost identical. However, comparison of ^{1}H NMR spectra from the product and a commercially available sample were identical.

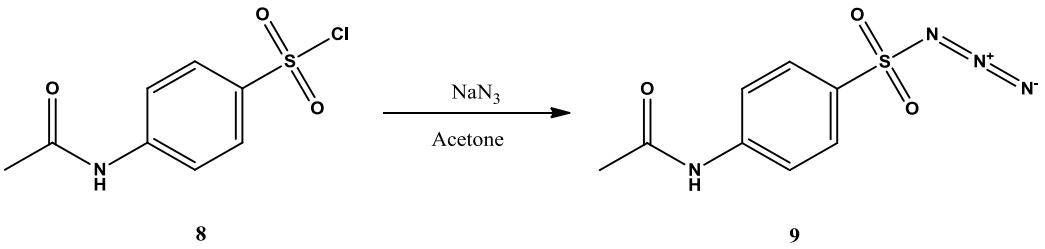

8 9

Equation 3: Synthesis of *p*-ABSA.

The next reaction was the production of dimethyl (diazomethyl)phosphonate (**11**), also known as the Seyferth/Gilbert reagent, for use in the synthesis of alkyne **6**. The procedure used was one published by Brown *et al.*[20] in 1996. Dimethyl methylphosphonate was added to a 250 mL flame-dried round-bottom flask containing THF under nitrogen. The solution was cooled to -78˚C and *n*-butyllithium was added dropwise over 5 minutes then allowed to stir for 30 minutes. 2,2,2-Trifluoroethylacetate was added rapidly and the solution was left to stir for 15 minutes. The mixture was allowed to warm to room temperature and partitioned between ether and 3 % HCl, then washed sequentially with saturated $NaHCO_3$ and saturated NaCl solutions. The organic layer was extracted, dried over $MgSO_4$, and the solvent was reduced to give dimethyl (3,3,3-trifluoro-2,2-dihydroxypropyl)-phosphonate which was immediately dissolved in anhydrous CH_3CN. *p*-ABSA was added and the mixture was cooled to 0˚C. Triethylamine was added dropwise over 5 minutes and the reaction was then allowed to warm to room temperature and left to react overnight. The solvent was removed under reduced pressure and chloroform was added to precipitate the byproduct 4-acetamidobenzenesulfonamide which was filtered of through a course glass frit. The filtrate was concentrated and purified through flash column chromatography with ethyl acetate to yield the phosphonate **11**. ^{1}H NMR showed one signal, a

doublet at 3.78 ppm corresponding to the methoxy protons, and ^{31}P NMR also showed a single signal at 22.33 ppm consistent with the single phosphorous atom.

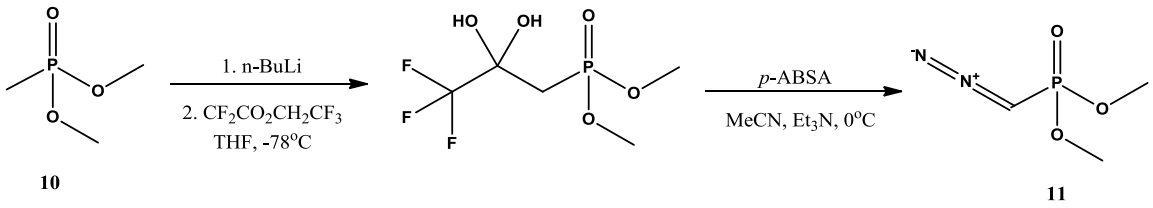

10 **11**

Scheme 3: Synthesis of dimethyl (diazomethyl)phosphonate **11**.

After the production of dimethyl (diazomethyl)phosphonate (**11**) the synthesis of alkyne **6** from aldehyde **5** was attempted. Potassium *tert*-butoxide was added to a 50 mL flame-dried round-bottom flask containing dry THF and then cooled to -78˚C. Dimethyl (diazomethyl)phosphonate (**11**) in dry THF was added to the flask and allowed to react for 5 minutes. Aldehyde **9** in dry THF was added and the solution was left to stir for 12 hours at -78˚C under nitrogen atmosphere. TLC showed the appearance of a new spot at a higher R_f value than the starting material. The ^1H NMR spectrum of the worked-up product was not clean and indicated that although the alkyne **6** was formed there were also signals present that corresponded to the starting materials. ESI mass spectrometry also confirmed the formation of the product **6** giving a mass of 446.2 which is consistent with the addition of sodium to the calculated mass of 423.13 amu.

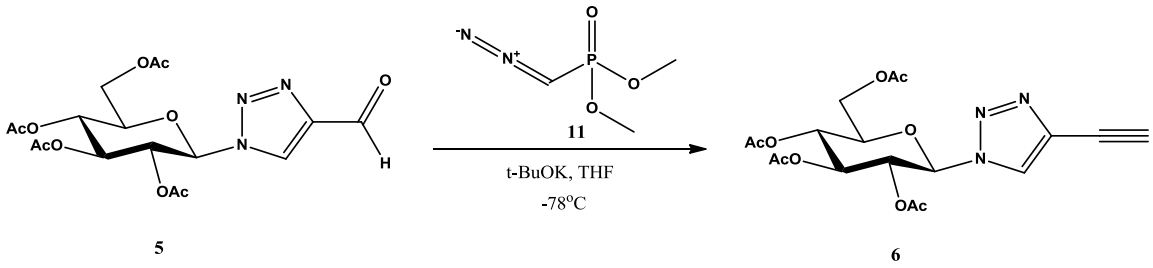

Equation 4: Synthesis of alkyne **6** from aldehyde **5** with **11** as a reagent.

Diethylacetylene dicarboxylate was reacted with azide **3** under reflux in toluene to produce triazole **11** as a single isomer without the use of a copper catalyst as in the other triazole syntheses (Equation 5). Upon completion TLC showed the formation of a new spot visible under UV light at a lower R_f value than the starting material. ^{1}H NMR confirmed the formation of the product with the shift of the anomeric proton's signal downfield from 4.64 to 6.13 ppm due to deshielding effects from the triazole. There were also several new signals from the carboxylate groups. There were two triplets at 1.41 and 1.43 ppm which correspond to the protons of the CH_3 groups of the dicarboxylate and two quartets at 4.43 and 4.48 ppm that correspond to the protons of the CH_2 groups.

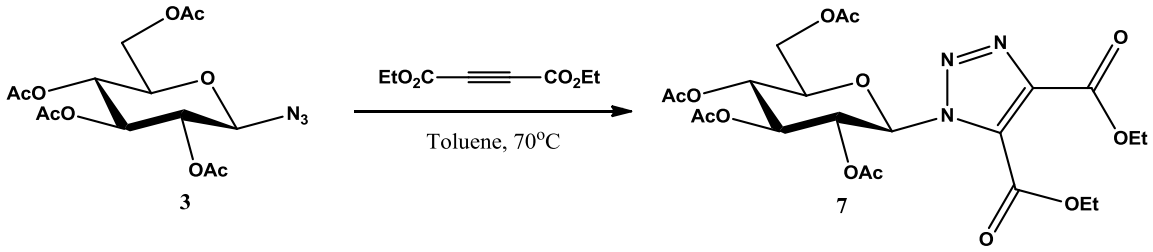

Equation 5: Synthesis of triazole **7** from azide **3**.

In order to test the effects of these compounds in biological systems the acetyl protecting groups must be replaced with the hydroxyl groups that would be found in nature. To this end compounds **3**, **4**, **7**, and dodecyne-derived triazole **13** were reacted with sodium methoxide in

methanol and the reaction was quenched with acidic ion exchange resin. The compounds were then recrystallized from ethanol or isopropanol to produce the hydroxylated compounds **13**, **14**, **15**, and **16** (Equations 6-9). Completion of the reactions was detected by the consumption of the starting materials with TLC. ^{1}H NMR spectra had many broad and overlapping signals due to the hydroxyl groups making it impossible to accurately assign most of the signals aside from the anomeric proton. In the case of the **16** single crystal x-ray data was also obtained which confirmed the structure and also exhibited some interesting packing qualities (Figure 11). It was observed (Figure 12) that because of the compound contained a polar region attached to a long non-polar hydrocarbon chain its molecules pack together in the same arrangement as a lipid bilayer.

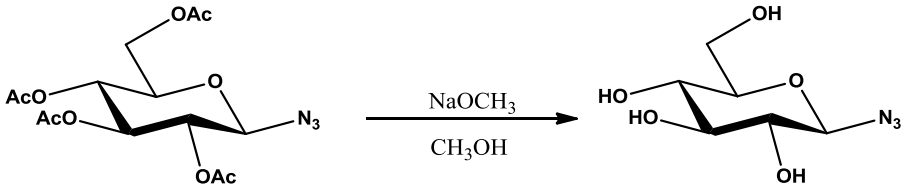

3 13

Equation 6: Deprotection of azide **3** to yield **13**.

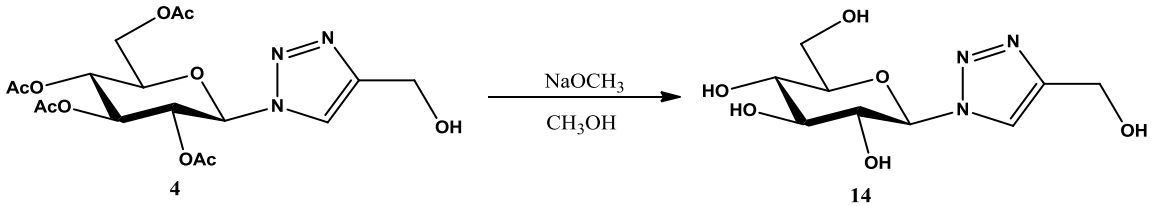

4 14

Equation 7: Deprotection of triazole **4** to yield **14**.

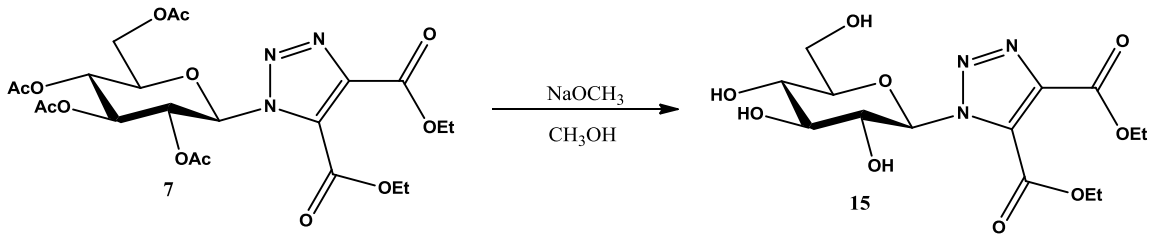

Equation 8: Deprotection of triazole **7** to yield **15**.

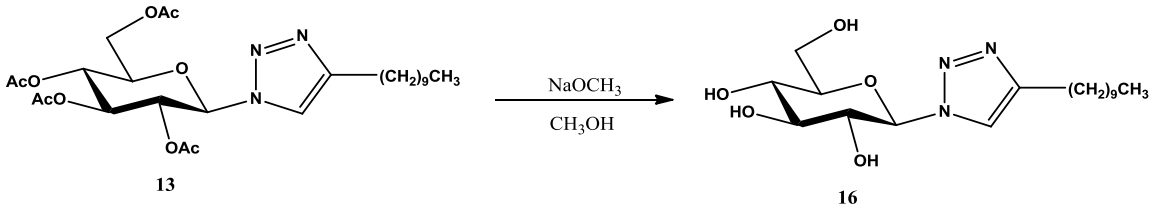

Equation 9: Deprotection of **13** to yield **16**.

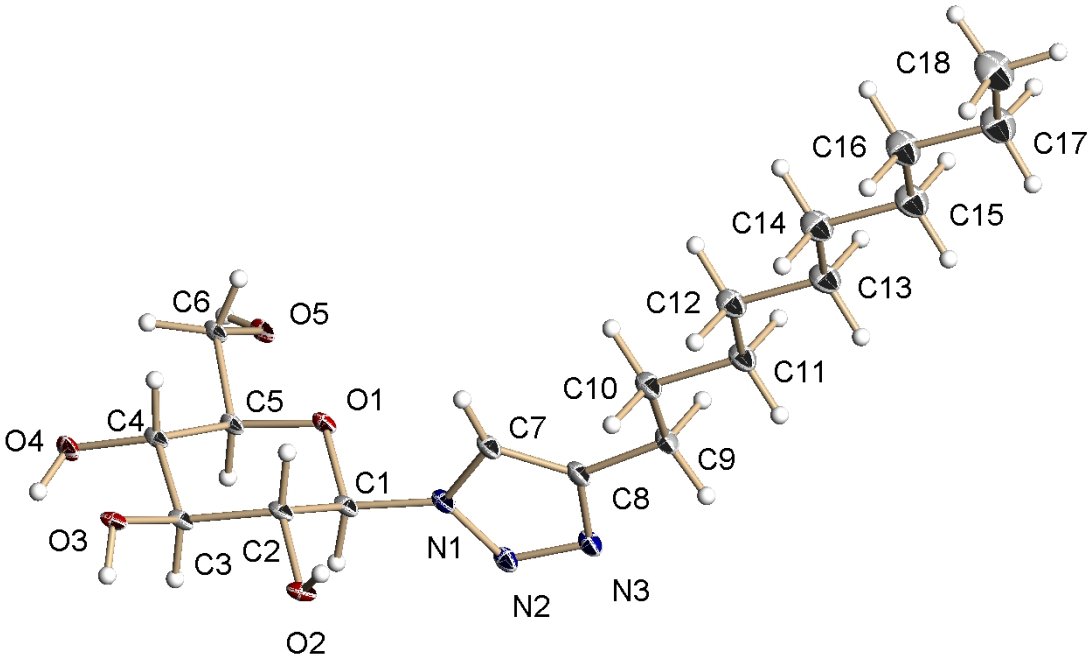

Figure 11: X-ray structure of deprotected dodecyne triazole **16**.

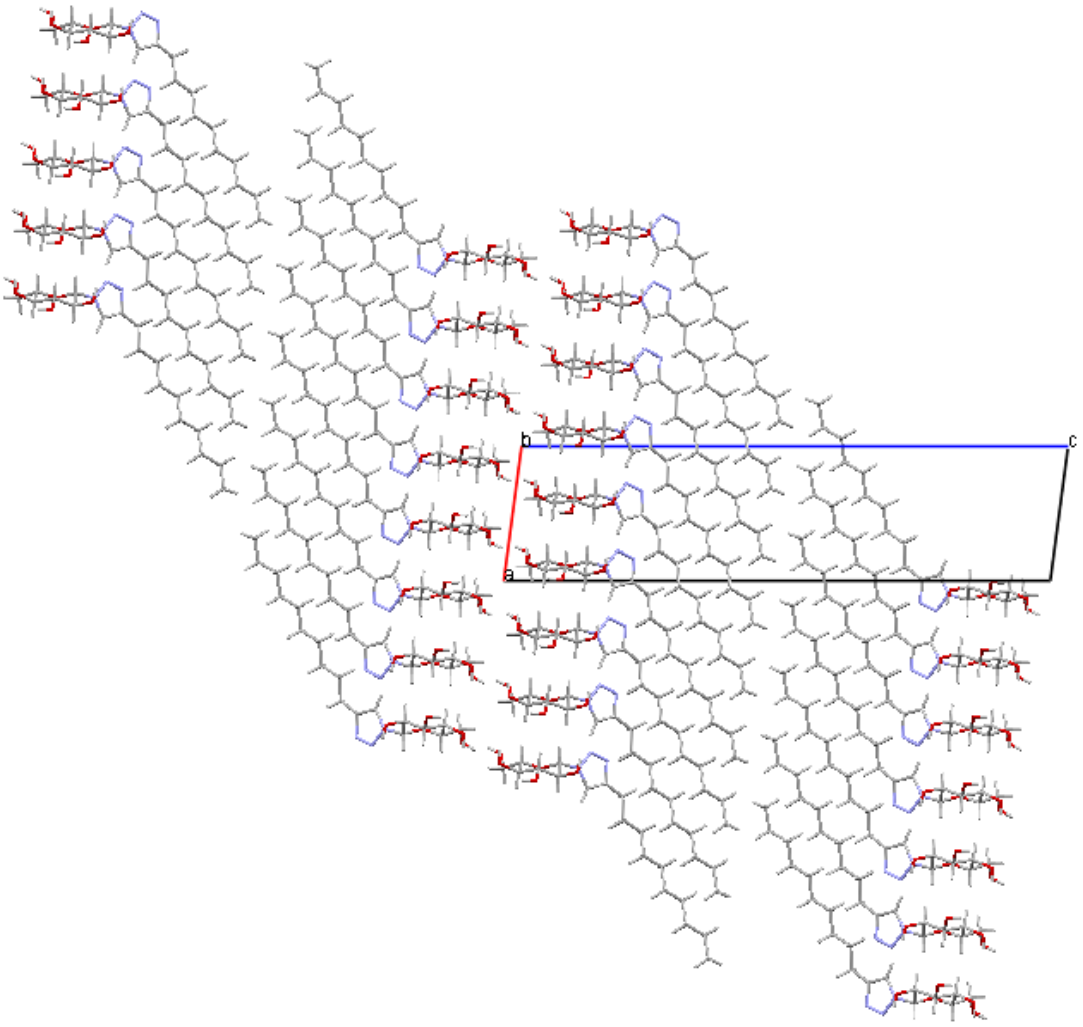

Figure 12: Packing view of deprotected dodecyne triazole **16**.

Biological Studies

Once deprotected, the sugar derivatives could be introduced into biological systems in order to test any effect they may exhibit. For this experiment we exposed C2C12 cells which are contractile muscle stem cells or myoblasts isolated from mice to a 0.06 mg/mL concentration of deprotected triazole **14**. The C2C12 cells were allowed to develop to the point of differentiation. From this point the cells were split into 6 control flasks and 3 flasks that would be given media containing compound **14** at a concentration of 0.06 mg/mL for 3 days and 3 that would be given

the treated media for 7 days before being harvested. The cells were observed with phase contrast microscopy daily throughout their development. No morphological differences were visible and both groups developed into the myotubes characteristic of this cell line. Both groups also exhibited intermittent twitching of the developing muscle fibers which indicates the development of normal functionality into contractile muscle.

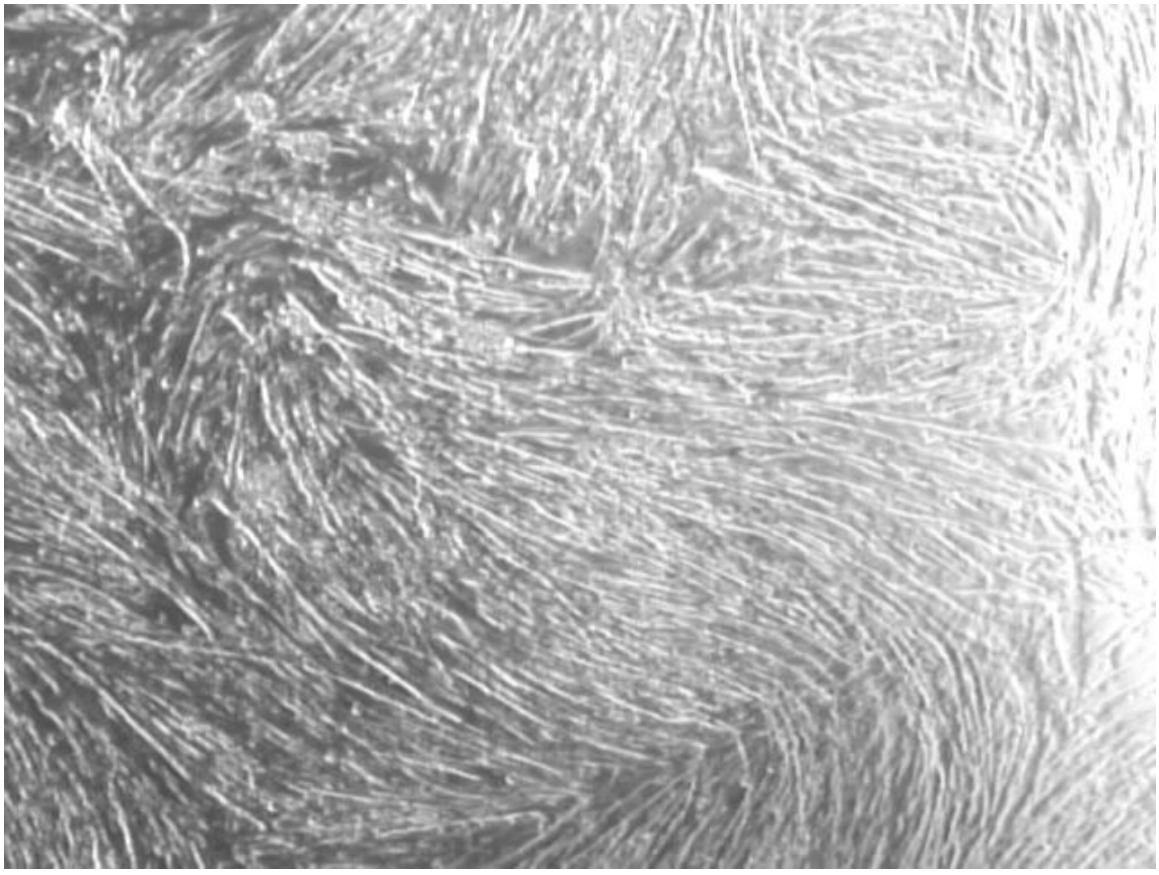

Figure 13: Control (non-treated) C2C12 muscle cells.

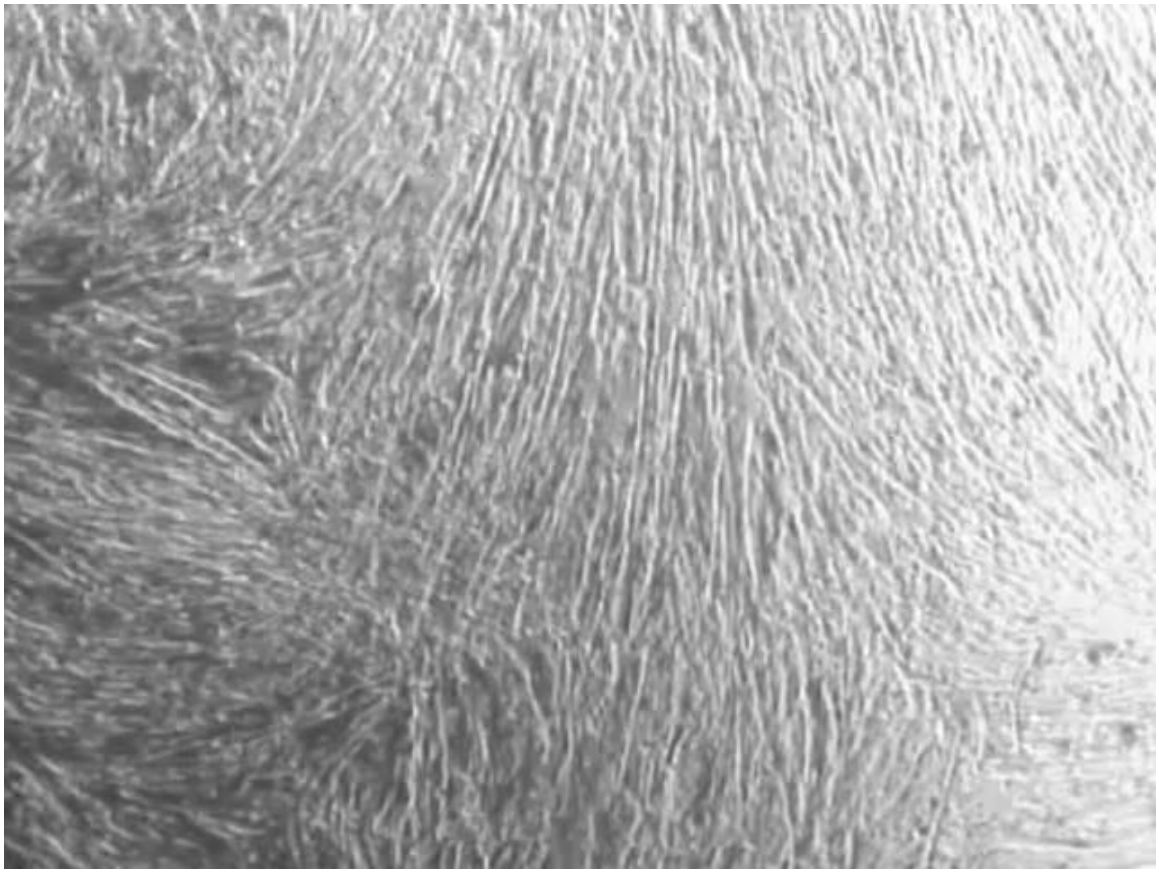

Figure 14: Treated C2C12 cells.

It may have been possible for compound **14** to be interacting with proteins in the cells in a manner that would alter their size or structure but was not affecting their functionality as contractile myotubes. For this reason SDS-PAGE was used to evaluate whether there were any differences in the protein profiles of the cells given media containing compound **14** when compared to those given the standard media. The samples were staggered with the treated samples next to their untreated counterpart for each time interval and a standard marker with bands at 176, 119, 75, 49, 39, 25, 19, 13, 10 kDa. Since compound **14** is much smaller and only has a molecular weight of 261.10 amu its presence will not appear on the gel unless it becomes bound to a larger protein.

Conclusion

After observing the gel it does not appear that there is any difference between the protein profiles of those cells given the treated media when compared to those that were given standard media (Figure 15). Each of the samples has the same pattern of bands indicating that compound **14** has not caused any alterations in the sizes of the proteins visible on the gel.

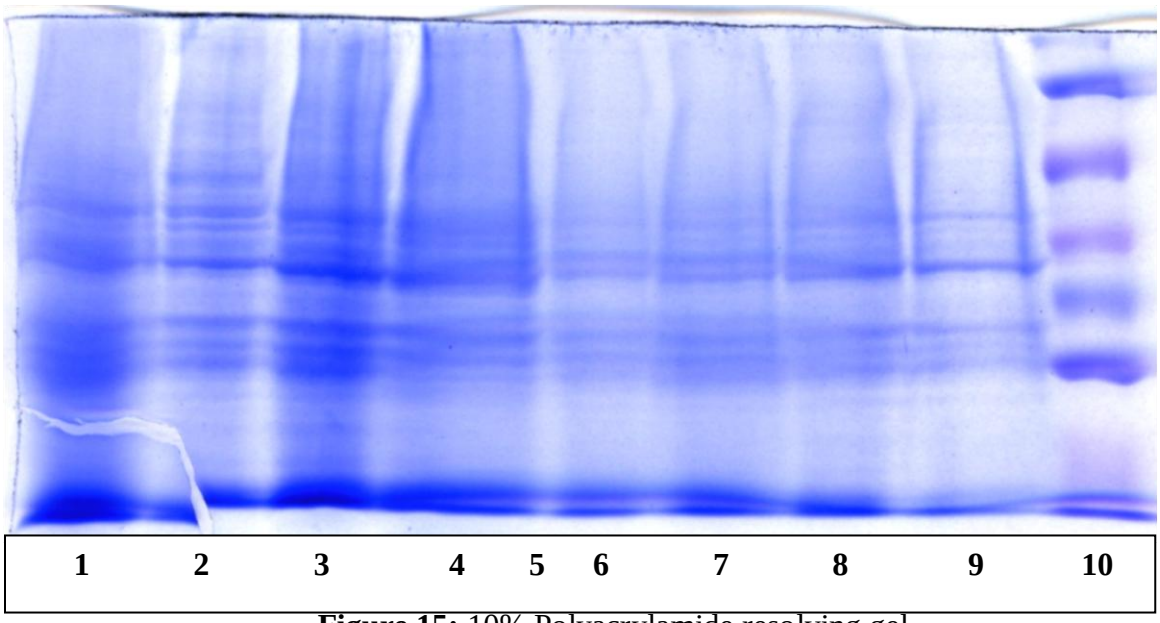

Figure 15: 10% Polyacrylamide resolving gel.

1	2	3	4	5	6	7	8	9	10
M.G. 3 day #14	M.G. 3 day control	M.G. 7 day #14	M.G. 7 day control	Empty	T.C. 3 day #14	T.C. 3 day control	T.C. 7 day #14	T.C. 7 day control	Standard

These results indicate that compound **14** at a concentration of 0.06 mg/mL when introduced into C2C12 cells in the manner used for this experiment had no effect on the protein profile of these cells. This was only a preliminary test to establish a protocol no definitive or broad conclusions can be established as to the effects of glycosyl triazoles on C2C12 stem cells in general. There are still many variables that have yet to be evaluated.

Future Work

The procedure established in this work for testing the effects of glycosyl triazoles on C2C12 cells can be greatly expanded. This experiment only included the testing of one compound at a single concentration. It is not known if the compound used in this experiment retains its structure when introduced into the media or the cells. It is possible that the compound may have some interaction with the media so it would be useful to do some studies on the stability of the compound in that environment to ensure the structure of the compound is retained when it is actually introduced into the cells. Another option may be to try a different method of introducing the compound into the cells. Future assays could also be developed to test the effects of varying concentrations of a single compound on these cells or to compare the effects of several different compounds. Although the current results indicated that the compound had no effect, future studies may find that at higher concentrations it will have some impact. If a higher concentration or different compounds do show some type of inhibition on the development or functionality of these cells further studies could be done to examine that effect in greater detail. For instance, another assay could be developed to test the compound's activity towards a particular enzyme present in these cells that may have been affected.

Experimental

Preparation of glucosyl bromide 2 from 1,2,3,4,6-penta-*O*-acetyl-*β*-D-glucose 1.

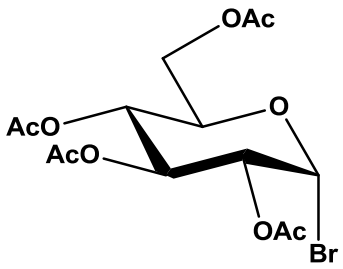

1,2,3,4,6-penta-*O*-acetyl-*β*-D-glucose (30.249 g, 77.5 mmol) was dissolved in 33% hydrobromic acid in acetic acid (120 mL) in a 250 mL round-bottom flask equipped with a stir bar. The reaction was allowed to stir for 3.5 hours until TLC showed consumption of the starting material. The solution was diluted with methylene chloride (150 mL) and cooled to 0˚C. The cold reaction mixture was then neutralized with 10% sodium hydroxide (480 mL) followed by aqueous saturated sodium bicarbonate (50 mL). The organic layer was extracted with methylene chloride (3 x 75 mL), dried over anhydrous magnesium sulfate, and gravity filtered. The remaining solvent was removed *in vacuo* to yield a white solid (30.960 g, 75.3 mmol, 97%).

^{1}H NMR ($CDCl_3$): δ 2.04, 2.06, 2.10, 2.11 (4s, 12H total, 4 x $COCH_3$), 4.23 (dd, 1H, H-6, *J* = 1.50, 12.18 Hz), 4.28-4.37 (m, 2H, H-5, H-6’), 4.85 (dd, 1H, H-2, *J* = 4.16, 10.20 Hz), 5.17 (dd, 1H, H-3, *J* = 9.82, 9.82 Hz), 5.56 (dd, 1H, H-4, *J* = 9.64, 9.88 Hz), 6.62 (d, 1H, H-1, *J* = 4.06 Hz).

Preparation of glucosyl azide 3 from glucosyl bromide 2.

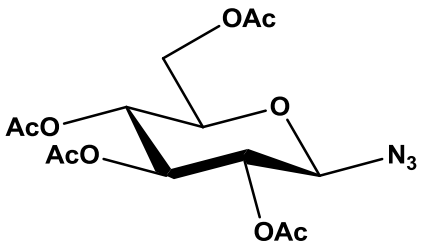

Sodium azide (22.745 g, 350 mmol) was added to a 1000 mL round-bottom flask equipped with a stir bar containing glucosyl bromide **1**(23.580 g, 57.3 mmol) dissolved in anhydrous *N*,*N*–dimethyl formamide (300 mL). The mixture was allowed to react overnight until TLC showed consumption of the starting material. Upon completion the reaction was washed with 5% Sulfuric acid (50 mL) followed by DI water (50 mL). The organic layers were extracted with methylene chloride (3 x 100 mL), dried over anhydrous magnesium sulfate, filtered and the solvent was reduced *in vacuo* to yield a white solid. The solid was recrystallized from hot methanol to produce rod-shaped clear crystals (20.902 g, 56.0 mmol, 98%).

^{1}H NMR ($CDCl_3$): δ 2.00, 2.03, 2.07, 2.10 (4s, 12H total, 4 x $COCH_3$), 3.79 (ddd, 1H, H-5, *J* = 2.35, 4.81, 10.05 Hz), 4.18 (dd, 1H, H-6, *J* = 2.30, 12.50 Hz), 4.28 (dd, 1H, H-6', *J* = 4.80, 12.45 Hz), 4.64 (d, 1H, H-1, *J* = 8.76 Hz), 4.96 (dd, 1H, H-2, *J* = 9.26, 9.44 Hz), 5.10 (dd, 1H, H-3, *J* = 9.74, 9.74 Hz), 5.22 (dd, 1H, H-4, *J* = 9.50, 9.50 Hz).

Preparation of glucosyl triazole alcohol 4 from glucosyl azide 3.

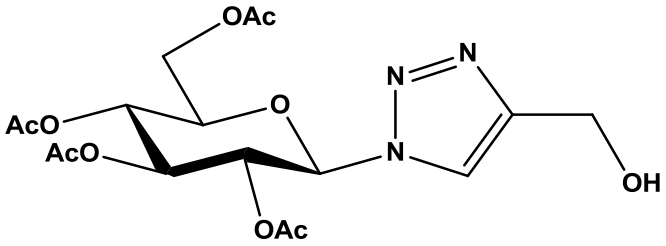

Glucosyl azide was added to a 200 mL round-bottom flask containing copper (II) sulfate (0.104 g, 0.40 mmol), ascorbic acid (1.036 g, 5.60 mmol), propargyl alcohol (2.00 mL, 33.9 mmol), 1:1 water:ethanol (50.0 mL), and equipped with a stir bar. The mixture was left to react overnight, then heated under reflux for 1 hour until TLC showed completion. The bulk of the solvent was removed under reduced pressure and the remainder was left to sit over the weekend in the remaining solvent. Crystals (3.039 g, 7.08 mmol, 70%) formed and were washed over a glass frit with cold DI water.

^{1}H NMR ($CDCl_3$): δ 1.89, 2.04, 2.08, 2.09 (4s, 12H total, 4 x $COCH_3$), 4.01 (ddd, 1H, H-5, *J* = 2.11, 5.01, 10.03 Hz), 4.15 (dd, 1H, H-6, *J* = 2.38, 12.66 Hz), 4.31 (dd, 1H, H-6', *J* = 4.90, 12.54 Hz), 4.82 (s, 2H, triazole-CH_2), 5.25 (dd, 1H, H-2, *J* = 9.86, 9.86 Hz), 5.42-5.45 (m, 2H, H-3, H-4), 5.86 (d, 1H, H-1, *J* = 9.24 Hz), 7.79 (s, 1H, triazole-H).

Preparation of glucosyl triazole aldehyde 5 from glucosyl triazole alcohol (4).

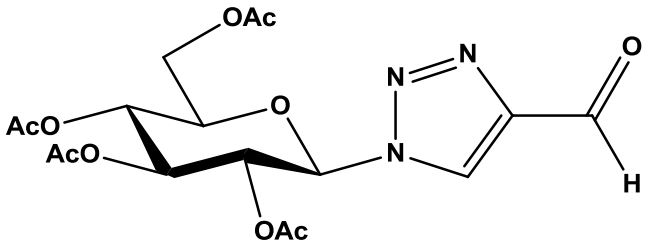

Glucosyl triazole alcohol (1.011 g, 2.33 mmol) was added to an oven-dried round-bottom flask equipped with a stir bar and containing pyridinium chlorochromate (2.961 g, 13.7 mmol), molecular sieves (3.003 g), and methylene chloride (55.0 mL). The mixture was left to react for 48 hours at room temperature until TLC showed completion. Molecular sieves were separated from the reaction mixture by filtration and some excess solvent was removed *in vacuo*. The resulting muddy brown syrup was then filtered through a wide silica column with ethyl acetate as the solvent. The appropriate fractions were collected and the solvent was reduced to produce a white solid which was then re-crystallized in hot methanol. (0.221 g, 0.52 mmol, 22 %)

^{1}H NMR ($CDCl_3$): δ 1.91, 2.04, 2.08, 2.10 (4s, 12H total, 4 x $COCH_3$), 4.03 (ddd, 1H, H-5, *J* = 2.17, 4.91, 10.25 Hz), 4.17 (dd, 1H, H-6, *J* = 2.20, 12.65 Hz), 4.32 (dd, 1H, H-6', *J* = 4.92, 12.76 Hz), 5.25 (dd, 1H, H-2, *J* = 9.16, 10.04 Hz), 5.38 (dd, 1H, H-3, *J* = 9.30, 9.30 Hz), 5.45 (dd, 1H, H-4, *J* = 9.30, 9.30 Hz) 5.93 (d, 1H, H-1, *J* = 9.32 Hz), 8.35 (s, 1H, triazole-H), 10.15 (s, 1H, aldehyde-H).

R_f = 0.52 (hexanes/ethyl acetate 1:3).

Preparation of glucosyl triazole alkyne 6 from glucosyl triazole aldehyde 5.

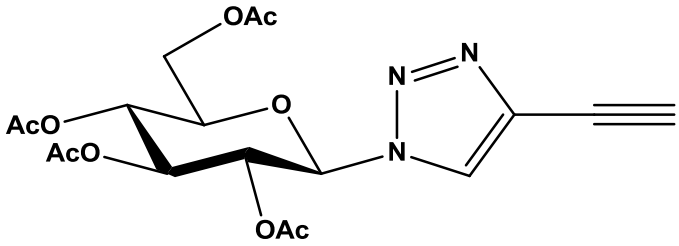

Potassium *tert*-butoxide (0.118 g, 1.68 mmol) was added to a 25 mL flame-dried round-bottom flask equipped with a magnetic stir bar and dissolved in anhydrous tetrahydrofuran (1.3 mL). The flask was flushed with nitrogen and cooled to -78 °C. Dimethyl(diazomethyl) phosphonate (**11**, 0.158 g, 1.05 mmol) in THF (1.8 mL), and glucosyl aldehyde (**4**, 0.310 g, 0.725 mmol) in THF (3.5 mL) were added to the flask and left to stir overnight at -78 °C under nitrogen. Upon completion the crude reaction mixture was diluted with DI water (25 mL) and extracted with methylene chloride (3 x 25 mL). The combined extracts were washed with brine (25 mL), dried over anhydrous magnesium sulfate, filtered, and the excess solvent was reduced. The product was further purified through flash column chromatography using 1:3 hexanes:ethyl acetate as a solvent. Isolation of the product was unsuccessful, however.

R_f = 0.57 (hexanes/ethyl acetate 1:3)

m/z calculated: 423.37 *m/z* found: 446.2 (+Na)

Preparation of glucosyl triazole dicarboxylate 7 from glucosyl azide 3.

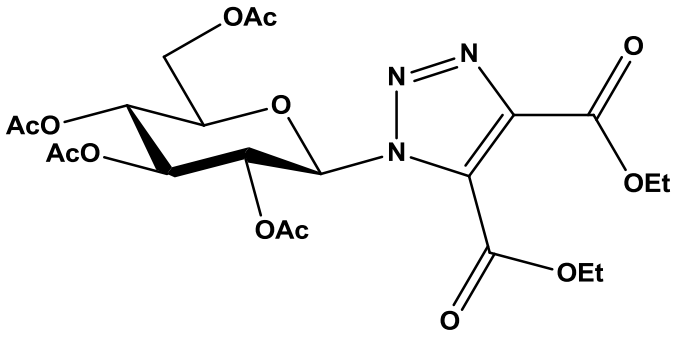

Glucosyl azide **3** (1.063 g, 2.85 mmol) was added to a 50 mL round-bottom flask equipped with a stir bar. Toluene (20.0 mL) and DEAD (1.00 mL, 6.25 mmol) were added to the flask and heated under reflux for 3 hours. The reaction was then left to react overnight until TLC showed consumption of starting material. The solvent was reduced and the crude product was recrystallized from hot ethanol to produce colorless crystals. (1.212 g, 2.23 mmol, 78% yield).

^{1}H NMR ($CDCl_3$): δ 1.41 (t, 3H, $CO_2CH_2C\underline{H}_3$, *J* = 7.02 Hz), 1.43 (t, 3H, $CO_2CH_2C\underline{H}_3$, *J* = 7.20 Hz), 1.90, 2.04, 2.06, 2.07 (4s, 12H total, 4 x $COCH_3$), 3.97 (ddd, 1H, H-5, *J* = 2.20, 4.90, 10.10 Hz), 4.14 (dd, 1H, H-6, *J* = 2.20, 12.76 Hz), 4.27 (dd, 1H, H-6', *J* = 4.82, 12.46 Hz), 4.43 (q, 2H, $CO_2C\underline{H}_2CH_3$, *J* = 7.04 Hz), 4.48 (q, 2H, $CO_2C\underline{H}_2CH_3$, *J* = 7.14 Hz), 5.25 (dd, 1H, H-2, *J* = 9.84, 9.84 Hz), 5.40 (dd, 1H, H-3, *J* = 9.52, 9.52 Hz), 5.97 (dd, 1H, H-4, *J* = 9.38, 9.38 Hz), 6.13 (d, 1H, H-1, *J* = 9.36 Hz).

R_f = 0.48 (hexanes/ethyl acetate 1:1).

Preparation of *p*-acetamidobezenesulfonyl azide 9) from *N*-acetyl sulfanilyl chloride (8).

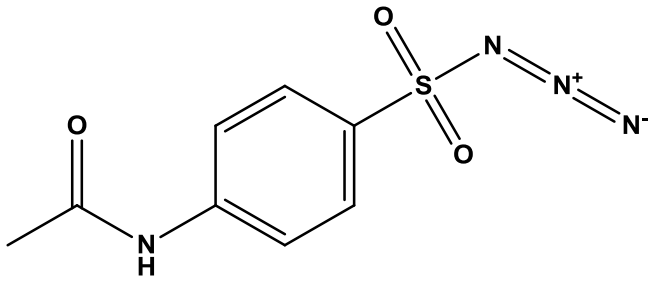

Sodium azide (5.710 g, 87.8 mmol) was added to a 1000 mL flame-dried round-bottom flask equipped with a stir bar and dissolved in acetone (400 mL). The mixture was cooled to 0˚C and *N*-acetyl sulfanilyl chloride (19.928 g, 85.3 mmol) was added in small portions over 5 minutes. The flask was flushed with nitrogen then left to react for 48 hours. Upon completion the reaction mixture was gravity filtered and the filtrate was concentrated to a yellowish-white crystalline solid (17.969g, 74.8 mmol, 88% yield).

^{1}H NMR ($CDCl_3$): δ 2.19 (s, 3H, CH_3), 2.25 (s, 1H, NH), 7.79 (d, 2H, Ar-H, *J* = 7.92 Hz), 7.91 (d, 2H, Ar-H, *J* = 8.68 Hz).

^{13}C NMR $CDCl_3$): δ 24.85, 31.026, 119.48, 129.06, 132.66, 143.88, 168.79, 207.39.

Preparation of dimethyl (diazomethyl) phosphonate (11) from dimethyl methyl phosphonate (10).

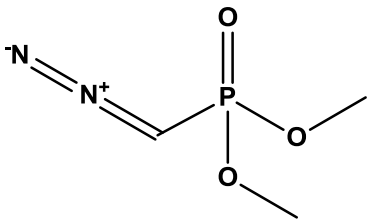

Anhydrous tetrahydrofuran (40 mL) was added to a flame-dried 250 mL round-bottom flask flushed with nitrogen. Dimethyl methyl phosphonate (2.00 mL, 18.4 mmol) was added and the solution was cooled to -78 °C. *n*-Butyllithium (11.47 mL, 18.4 mmol) was added dropwise over 5 minutes and left to stir at -78 °C for 30 minutes. 2,2,2-trifluoroethyl trifluoroacetate (3.73 mL, 27.6 mmol) was added rapidly and the reaction was left to stir for 15 minutes at -78 °C. The solution was allowed to warm to room temperature and then partitioned between ether (25 mL) and 3% hydrochloric acid (10 mL). The organic layer was washed with saturated sodium bicarbonate (10 mL) followed by saturated sodium chloride (10 mL). The organic layers were dried over anhydrous magnesium sulfate and gravity filtered. Excess solvent was removed from the filtrate *in vacuo* to yield 3,3,3-trifluoro-2,2-dihydroxypropyl phosphonate as a yellow oil. This crude product was then immediately dissolved in anhydrous acetonitrile (40 mL) and *p*-acetamidobenzenesulfonyl azide was added. The reaction was cooled to 0 °C and triethylamine was added dropwise over 5 minutes. The reaction was allowed to warm to room temperature and left to react overnight. The solvent was then reduced and chloroform was added to precipitate 4-acetamidobenzenesulfonamide. The slurry was filtered through a course glass frit and the filtrate was concentrated to an orange oil. The crude product was then further purified through flash column chromatography with ethyl acetate and the fractions evaporated.

^{1}H NMR ($CDCl_3$): δ 3.78 (d, 2 x OCH_3, J = 11.80 Hz).

^{31}P NMR ($CDCl_3$): δ 22.33.

Typical procedure for the deprotection of acetyl-protected sugars 3, 4, 7, and 12 to yield 13, 14, 15 and 16.

A small piece of a sodium pellet was added to a dry Erlenmeyer flask containing methanol (5 mL). The acetyl-protected sugar **3**, **4**, **7**, or **12** (1 mmol) was added to a 50 mL round-bottom flask containing methanol (10 mL) and equipped with a stir bar. Once the sodium pellet had completely dissolved to form sodium methoxide the contents of the Erlenmeyer flask were slowly added to the round-bottom flask containing the sugar. The mixture was then capped with a septum, vented with a needle, and left to stir for 2 hours. Acidic amberlite exchange resin (1.00 g) was added and left to stir for 1 hour. The resin was filtered off and the solvent was reduced to give compounds **13**, **14**, **15**, and **16** as crystalline solids.

Deprotected glucosyl azide 13.

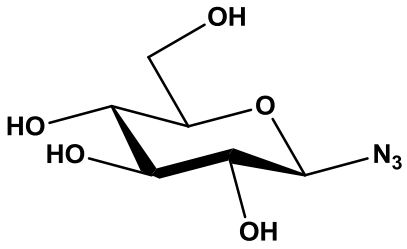

R*f* = 0.11 (ethyl acetate).

Deprotected triazole alcohol 14.

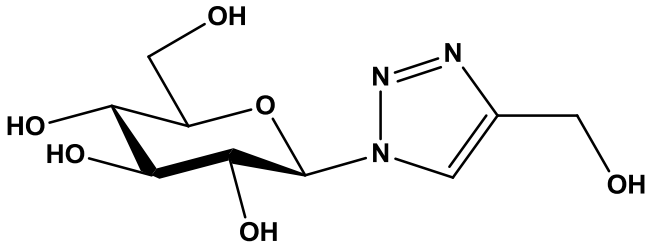

R*f* = 0.01 (ethyl acetate).

Deprotected triazole dicarboxylate 15.

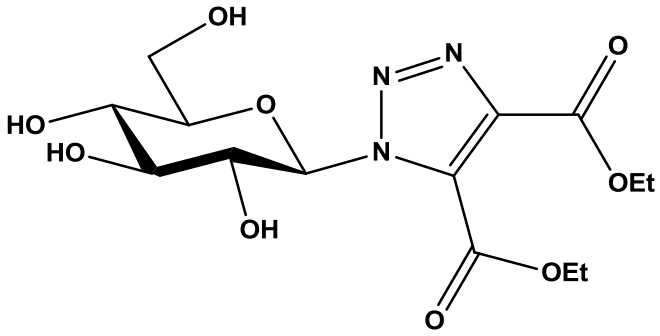

R*f* = 0.60 (methanol/ethyl acetate 1:1).

Deprotected triazole dodecyne 16.

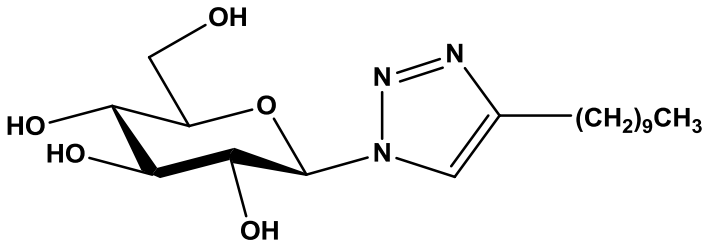

R_f = 0.15 (ethyl acetate).

C2C12 Cell Culture

Complete media was prepared by adding 55.0 mL of fetal bovine serum and 5.5 mL of penicillin-streptomycin to 500 mL of Dulbecco's modification of eagle's medium with 4.5 g/L glucose and L-glutamine without sodium pyruvate (DMEM) in a non-sterile environment. The media was then sterilized through a 0.22 μm Corning® bottle-top vacuum filter in a sterilized laminar flow hood.

A 1.0 mL vial of C2C12 cells were thawed rapidly to 37 °C from storage in liquid nitrogen in a hot water bath. Once thawed, cells were transferred to a centrifuge tube under sterile conditions. Approximately 2.0 mL of complete media was added to the centrifuge tube and left for 5 minutes. Another 2.0 mL portion of media was added and left to sit for an additional 5 minutes. Then a 4.0 mL portion of media was added and again left to sit for 5 minutes. At this point the entire contents of the centrifuge tube (~10 mL) followed by 50 mL of complete media were transferred to cap-vented, Corning® CellBIND® cell culture flask with a surface area of 150 cm^2 under sterile conditions. The flask was immediately placed in an incubator set at 37 °C and observed periodically with phase contrast microscopy during the next

24 hours for signs of attachment. Cells were left to multiply and divide for an additional 3 days and were observed once a day during this period to ensure normal growth. On the fifth day the cells were sub-cultured into five 75 cm^2 culture flasks. In a sterile laminar flow hood, the mother flask was rinsed several times with 25-50 mL portions of incomplete media and 25 mL of complete media is added to each of the five smaller flasks. Approximately 15 mL of 0.25% trypsin/EDTA was added to the mother flask and left to incubate at 37 °C for 10 minutes. The flask was removed from the incubator and the side of the flask was sharply rapped in order to encourage detachment. Detachment is confirmed by the cloudy appearance of the fluid in the flask. The detached cells were transferred to a 15 mL centrifuge tube and 25 mL of complete media was added to the mother flask and it was returned to the incubator. A 3 mL portion of the detached cell solution was added to each of the 5 new culture flasks and they were placed in the incubator. Again, the flasks were monitored periodically for the next 24 hours for attachment. It was observed that the cells required further subculture and were transferred into twenty-four 25 cm^3 culture flasks. The procedure for this was the same as the first subculture except that the 75 cm^3 flasks were rinsed with 25 mL of incomplete media, only 10 mL of complete media were added to each of the new flasks, the detached cells were transferred to a 50 mL centrifuge tube, and 1 mL of the detached cell solution was added to each of the new flasks. From this point on the cells were observed and videotaped everyday and given fresh media (or fed) every 3 days for 12 days. Differentiation media and treated differentiation media were prepared. The former was prepared by adding 55.0 mL of FBS to an unopened 500 mL bottle of DMEM. The treated media was prepared by dissolving 0.600 g of **14** in 1.00 mL of DMSO (dimethyl suloxide) which was further diluted to a concentration of 0.06 mg/mL with the previously prepared differentiation media. At this point the 24 flasks were divided up for use in two different

experiments with 12 flasks used in each. The 12 flasks were further split into 6 control flasks and 6 treated flasks. The 6 control flasks were fed every three days with differentiation media and the treated flasks were fed with the differentiation media containing a 0.06 mg/mL concentration of **14**. As before the cells were observed and videotaped everyday with phase contrast microscopy. One of the treated flasks became contaminated and was removed from the experiment. Three of the treated flasks and three of the control flasks were harvested after 3 days and stored at 0 °C. The remaining three control flasks and two treated flasks were harvested after 7 days. The cells were harvested by first pouring off the old media from each of the flasks. Approximately 1 mL of PBS solution was used to rinse remaining media from each flask. Then 0.5 mL of 1X SDS-PAGE solution was added to each flask to detach the cells. Each flask was swirled until all the cells appeared to have detached and concentrated in the SDS-PAGE solution. The cells from each flask were then carefully transferred into separate labeled 1.8 mL snap-cap microfuge tubes which were stored in the freezer. Once all the cells had been harvested they were loaded onto a SDS-PAGE gel.

SDS-PAGE

A 5% Acrylamide stacking gel was prepared by mixing and swirling stacking gel buffer (1.13 mL), distilled water (2.65 mL), and 40% stacking acrylamide (0.75 mL) together in a 25 mL Erlenmeyer flask. A glass gel plate was propped up at a slight angle and a pre-made 10% polyacrylamide gel was laid across it. Next, 10 % APS (15 µL) and TEMED (5.75 µL) were added to the 25 mL Erlenmeyer and swirled into the rest of the solution. This stacking gel solution was carefully inserted between the glass plate and the pre-made gel. A comb was then carefully inserted into the top of the stacking gel and it was left to set. In the meantime the

electrophoresis apparatus was assembled and the chambers were filled with electrophoresis running buffer. Once the stacking gel set the comb was removed to give a gel with 10 lanes. The fifth lane was left empty and lanes 6-9 were filled with 10 µL each of the current samples and the last lane was filled with 8 µL of a standard marker.

1	2	3	4	5	6	7	8	9	10
M.G. 3 day #14	**M.G. 3 day control**	**M.G. 7 day #14**	**M.G. 7 day control**	**Empty**	**T.C. 3 day #14**	**T.C. 3 day control**	**T.C. 7 day #14**	**T.C. 7 day control**	**Standard**

The gel was run at 20 mA for 2 hours and 34 minutes. The gel was then carefully removed from the electrophoresis apparatus and stained overnight in coomassie brilliant blue R-250. The gel was then soaked in high destain for 1 hour followed by low destain for 1 hour. When scanned after this procedure the gel still appeared a little wet making the image a little hazy so it was dried overnight in 5% acetic acid, then left for another 24 hours in a drying frame between two sheets of cellulose.

References

1. Berendse, M.; Grounds, M.D.; Lloyd, C.M. Myoblast Structure Affects Subsequent Skeletal Myotube Morphology and Sarcomere Assembly. *Exp. Cell Res.* **2003,** 291, 435-450.

2. Coward, S. J. "Developmental Regulation: Aspects of Cell Differentiation." Academic Press: New York, **1973.**

3. Healy, E. F. *Myosin Structure Web Page* [Online]: St. Edwards University Department of Chemistry. (accessed June 7, 2010) http://www.cs.stedwards.edu/chem/Chemistry/CHEM43/CHEM43/Myosin/STRUCT~1.HTM

4. Zelinka, L. M. The Immunofluorescent Localization of Antigens Associated with Rippling Muscle. M.S. Thesis, Youngstown State University, Youngstown, OH, 2002.

5. Spizz, G.; Roman, D.; Strauss, A.; Olsen, E. N. Serum and fibroblast growth factor inhibit myogenic differentiation through a mechanism dependent on protein synthesis and independent of cell proliferation. *J. Biol.Chem.***1986**, 261, 9483-9488.

6. Olsen, E. N.; Sternberg, E.; Hu, J.S.; Spizz, G.; Wilcox, C. Regulation of myogenic differentiation by type beta transforming growth factor. *J. Cell Biol.* **1986**, 103, 1799-1805.

7. Clegg, C. H.; Linkhart, T. A.; Olwin, B. B.; Hauschka, S. D. Growth factor control of skeletal muscle differentiation occurs in G1-phase and is repressed by fibroblast growth factor. *J. Cell Biol.* **1987**, 105, 949-956.

8. Tajbakhsh, S. Skeletal muscle stem cells in development versus regenerative myogenesis. *J. Intern. Med*. **2009**, 266, 372-389.

9. Duan, C.; Ren, H.; Gao, S. Insulin-like growth factors (IGFs), IGF receptors, and IGF-binding proteins: roles in skeletal muscle growth and differentiation. *Gen. Comp. Endocr.* **2010**, 167, 344-351.

10. Olsen, E. N.; Brennan, T. J.; Chakraborty, T.; Cheng, T.; Cserjesi, P.; Edmondson, D.; James, G.; Li, L. Molecular control of myogenesis: antagonism between growth and differentiation. *Mol. Cell. Biochem.* **1991**, 7-13.

11. Lackie, J.M.; Dow, J.A.T. "The Dictionary of Cell and Molecular Biology." Academic Press: London, **1999.**

12. Voet, D., Voet, J. G., Pratt, C., W., "Fundamentals of Biochemistry." John Wiley & Sons: New York, **2002**.

13. Stick, R. V. "Carbohydrates: The Sweet Molecules of Life." Academic Press: London, **2001**.

14. Vicarel, M. L. Synthesis of N-Glycosides Using Azidodeoxysugars. M.S. Thesis, Youngstown State University, Youngstown, OH, 2006.

15. Collins, P. M.; Ferrier, R. J. "Monosaccharides: Their Chemistry and Their Roles in Natural Products." John Wiley & Sons: West Sussex, **1995**.

16. Anagnostou, E.; Kosmopoulou, M. N.; Chrysina, E. D.; Leonidas, D. D.; Hadjiloi, T.; Tiraidis, C.; Zographos, S. E.; Györgydeák, Z.; Somsák, L.; Docsa, T.; Gergerly, P.; Kolisis, F. N.; Oikonomakos, N. G. Crystallographic studies on two bioisosteric analogues, *N*-acetyl-β-D-glucopyranosylamine and *N*-trifluoroacetyl-β-D-glucopyranosylamine, potent inhibitors of muscle glycogen phosphorylase. *Bioorg. Med. Chem.* **2006**, 14, 181-189.

17. Hadjiloi, T,; Tiraidis, C.; Chrysina, E. D.; Leonidas, D. D.; Oikonomakos, N. G.; Tsipos, P.; Gimisis, T. Binding of oxalyl derivatives of b-D-glucopyranosylamine to muscle glycogen phosphorylase b. *Bioorg. Med. Chem.* **2006**, 3872-3882.

18. Czifrák, K.; Hadady, Z.; Docsa, T.; Gergely, P.; Schmidt, J.; Wessjohann, L.; Somsák, L. Synthesis of *N*-(b-D-glucopyranosyl) monoamides of dicarboxylic acids as potential inhibitors of glycogen phosphorylase. *Carbohydr. Res.* **2006**, 341, 947-956.

19. Bock, V. D.; Hiemstra, H.; van Maarseveen, J. H. Cu^{I}-catalyzed alkyne-azide "click" cycloadditions from a mechanistic and synthetic perspective. *Eur. J. Org. Chem.* **2006**, 51-68.

20. Brown, D. G.; Velthuisen, E. J.; Commerford, J. R.; Brisbois, R. G.; Hoye, T. R. A convenient synthesis of dimethyl (diazomethyl)phosphonate (Seyferth/Gilbert reagent). *J. Org. Chem.* **1996**, 2540-2541.

Appendix A

NMR & Mass Spectra

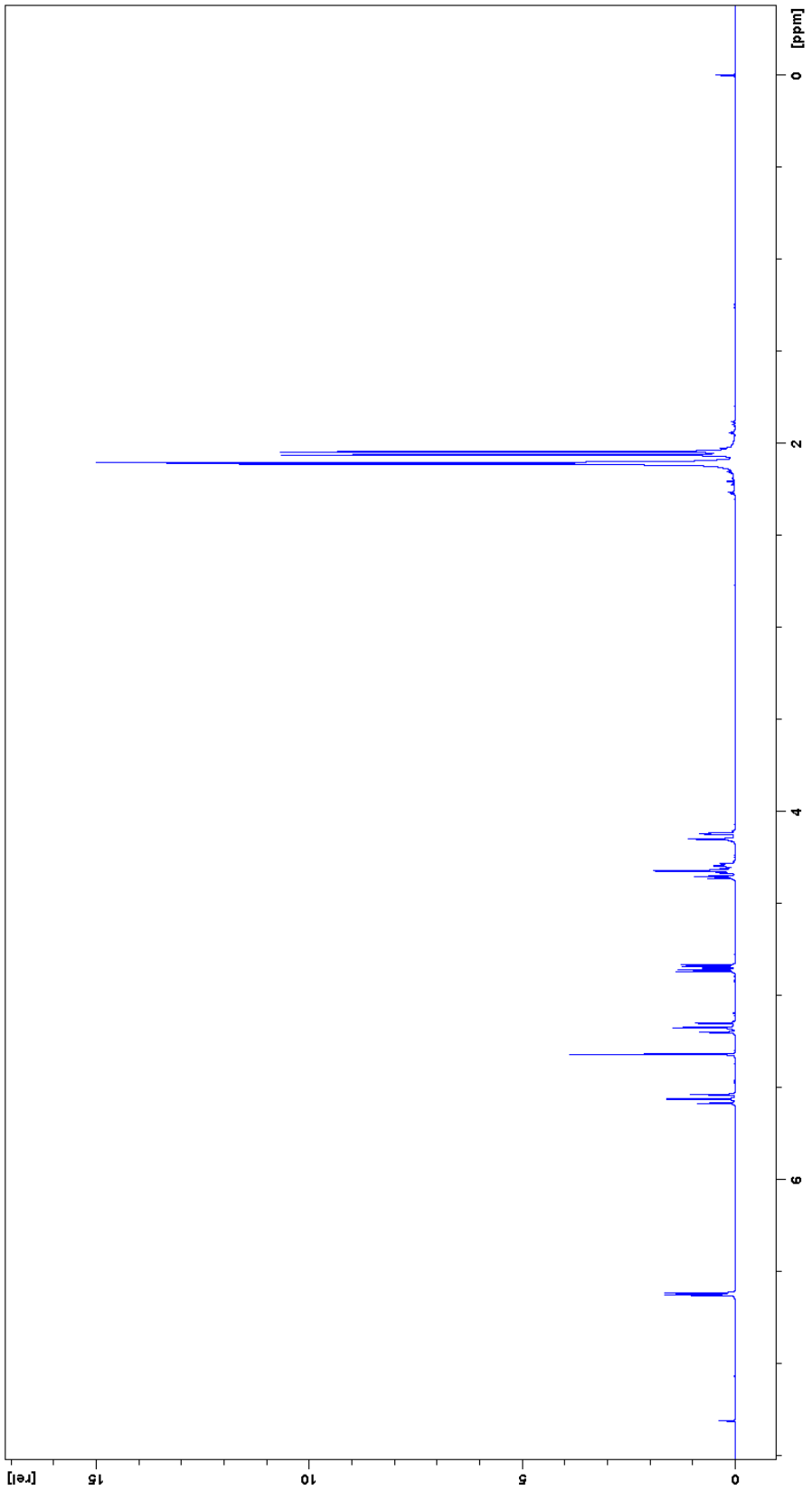

Figure 16: 400 MHz ^{1}H spectrum of glucosyl bromide **2.**

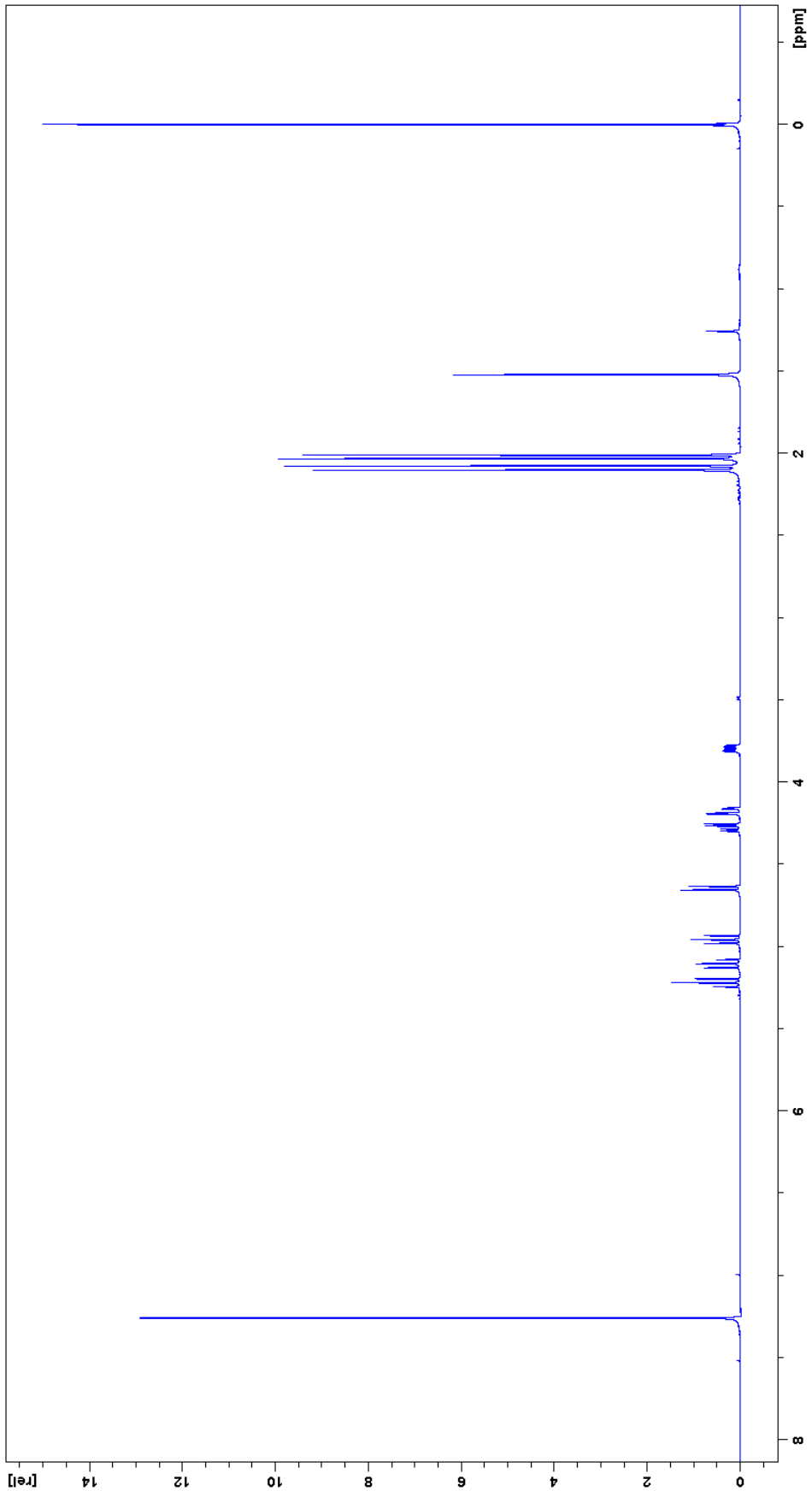

Figure 17: 400 MHz ^{1}H spectrum of glucosyl azide **3**.

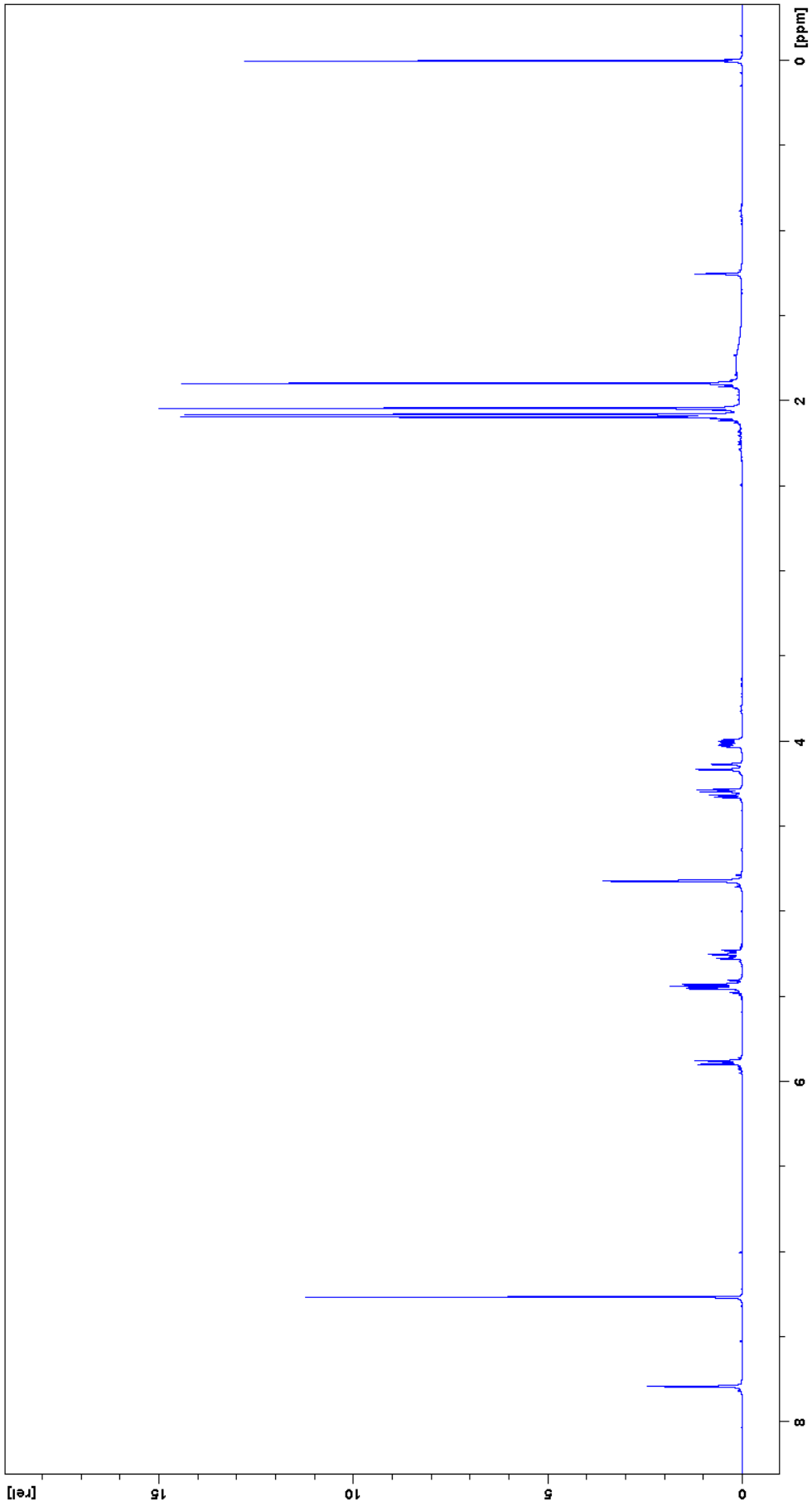

Figure 18: 400 MHz ^{1}H spectrum of glucosyl triazole **4**.

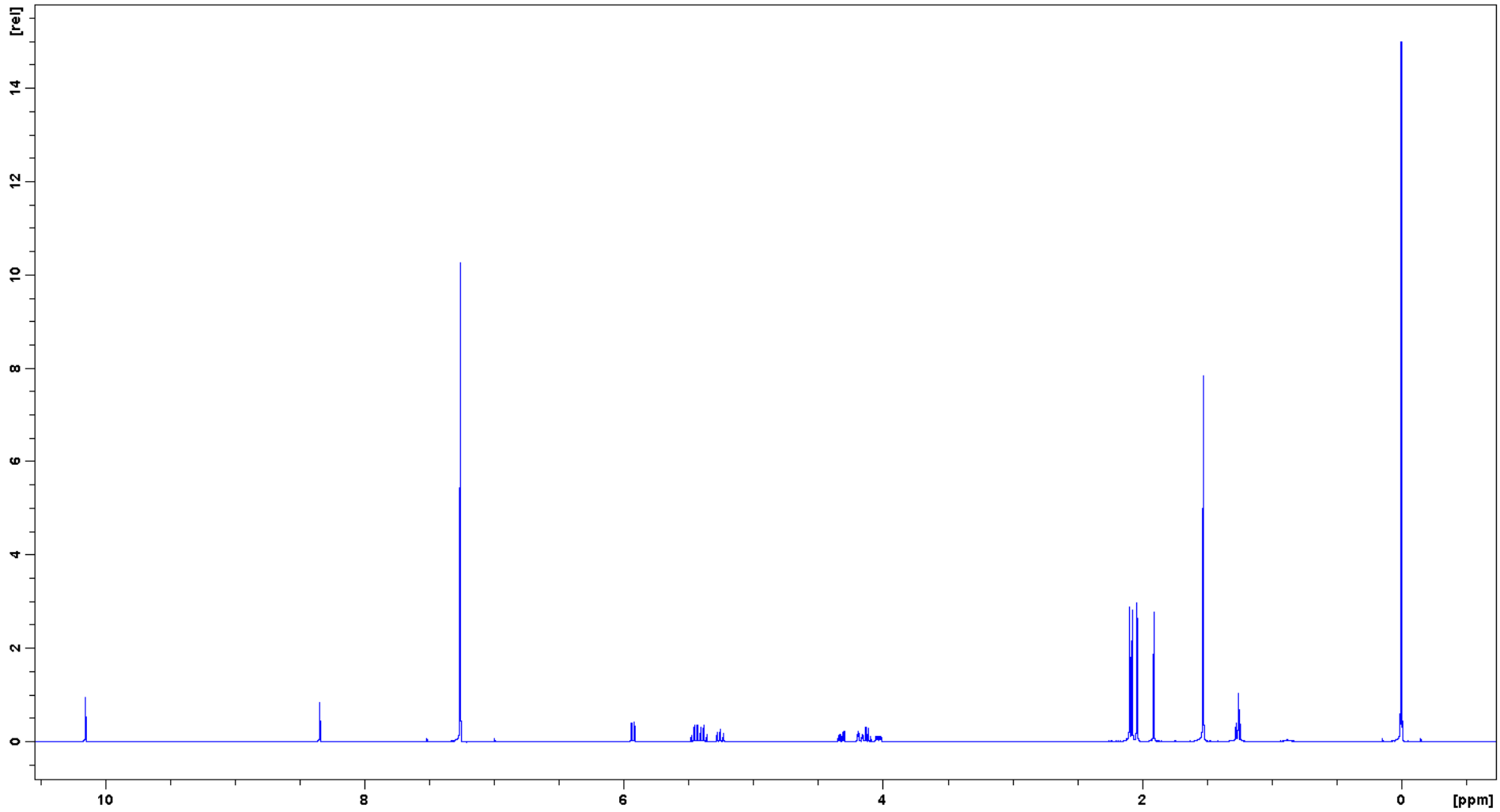

Figure 19: 400 MHz ^{1}H spectrum of glucosyl triazole **5**.

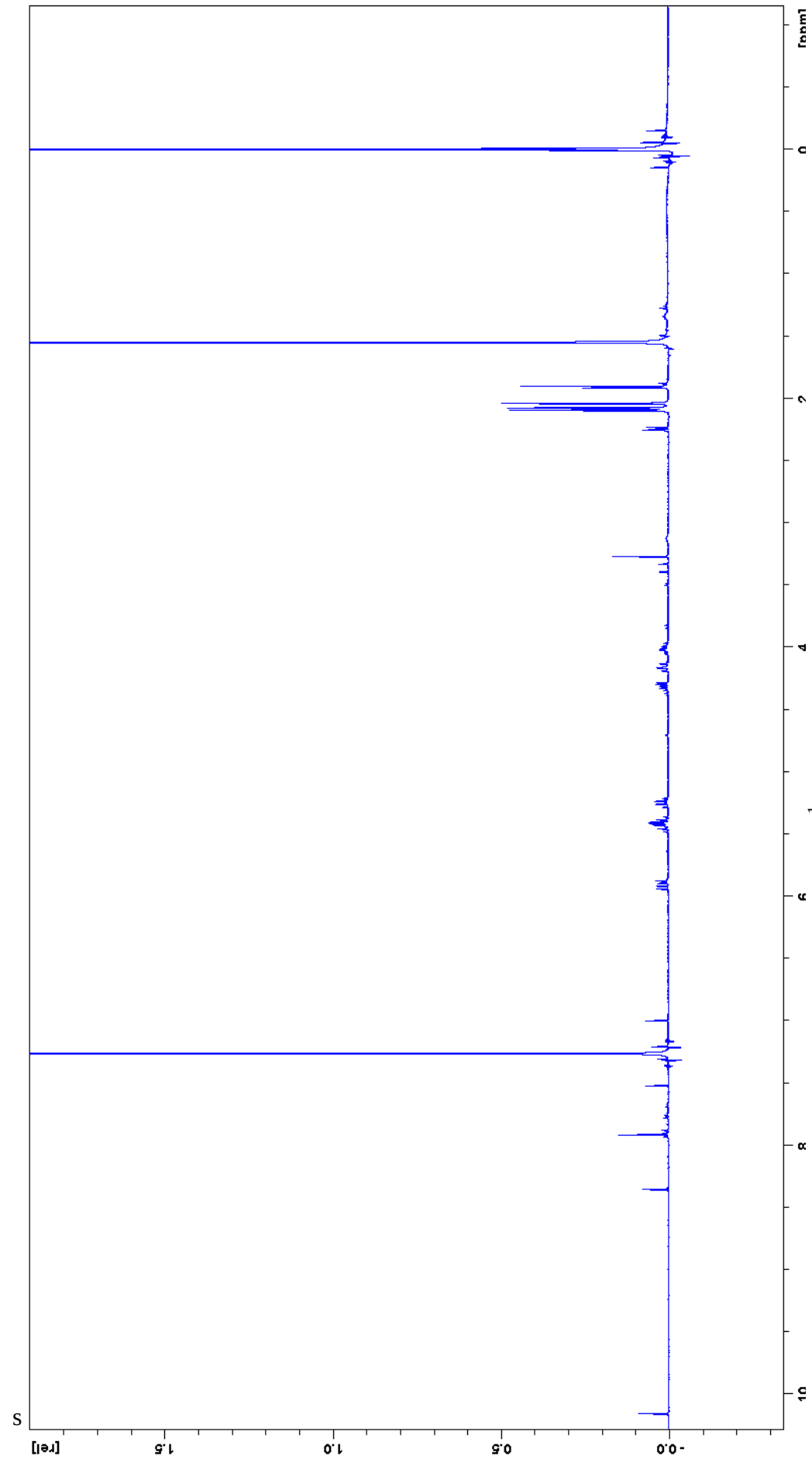

Figure 20: 400 MHz ^{1}H spectrum of glucosyl triazole **6**.

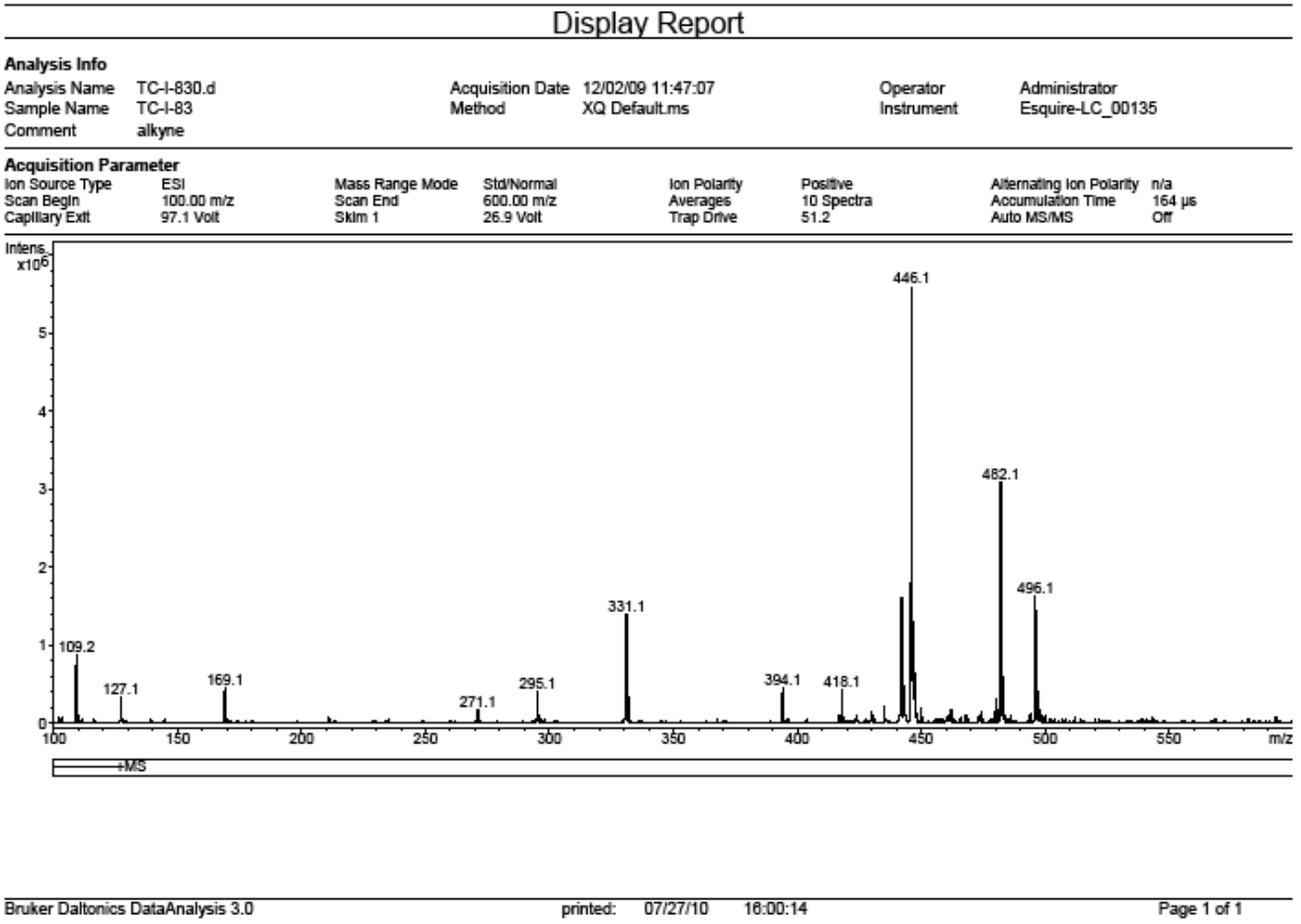

Figure 21: Mass spectrum of glucosyl triazole **6**.

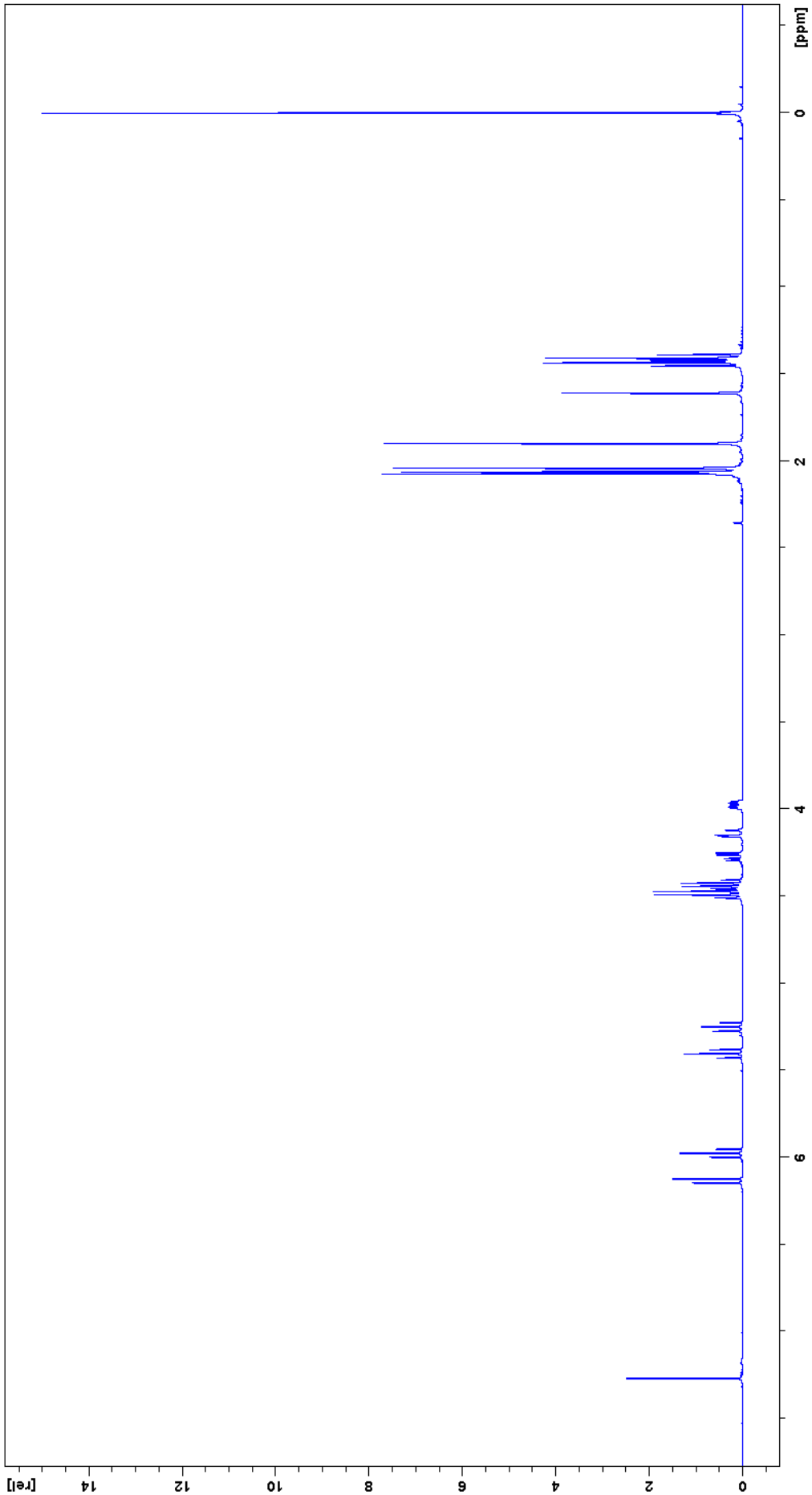

Figure 22: 400 MHz ^{1}H spectrum of glucosyl triazole **7**.

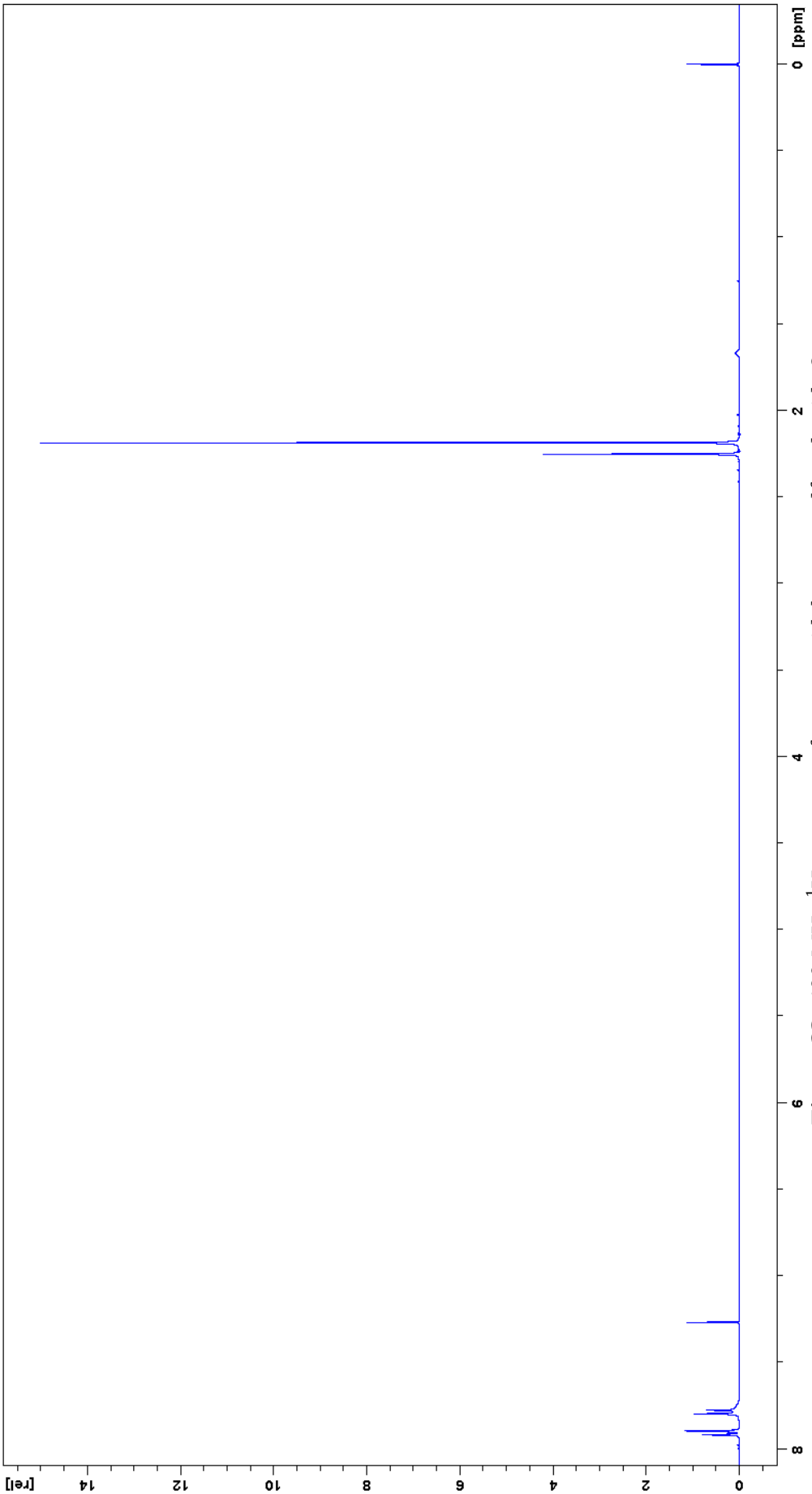

Figure 23: 400 MHz ^{1}H spectrum of *p*-acetamidobenzenesulfonyl azide **9**.

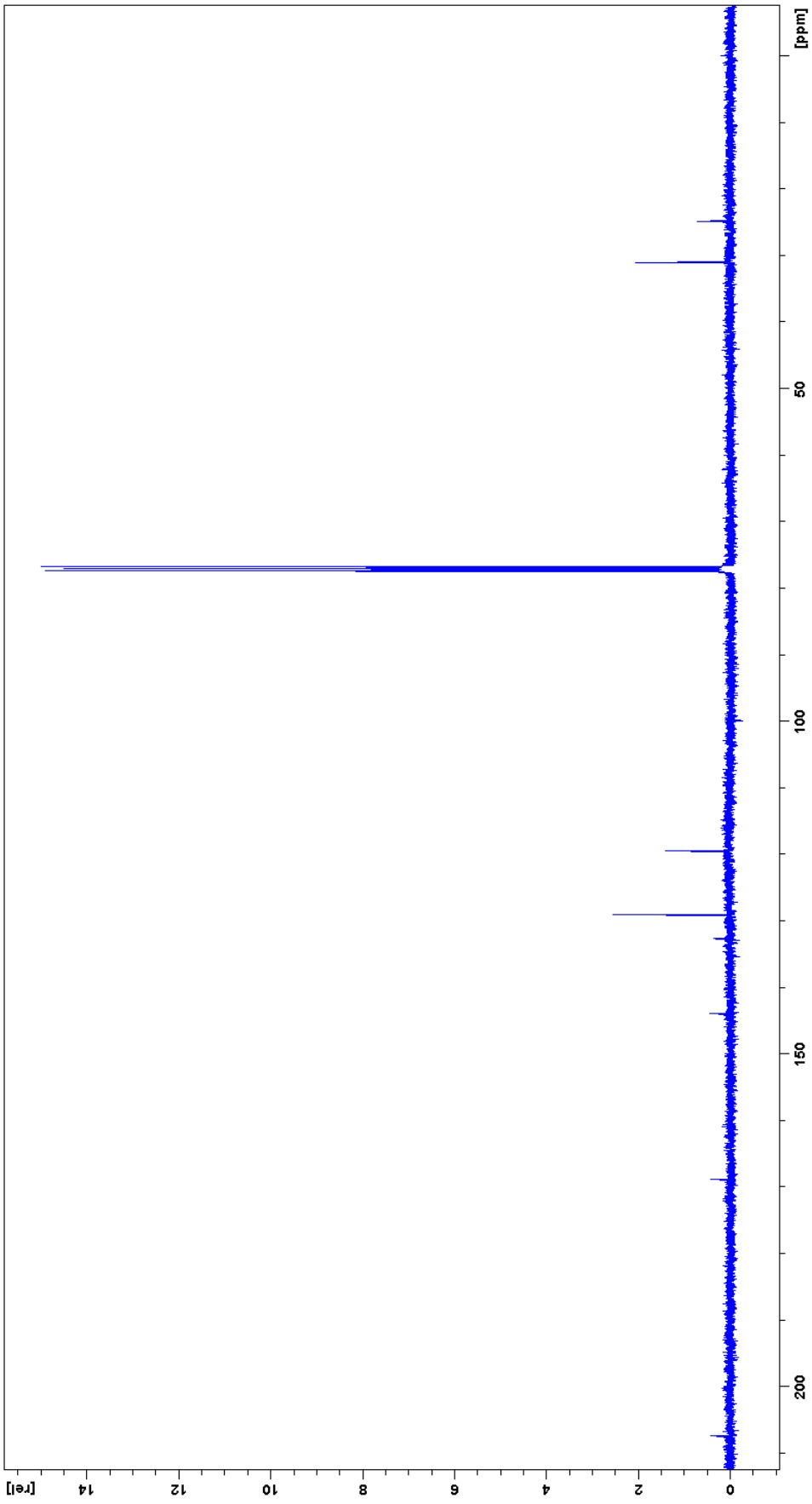

Figure 24: 100 MHz ^{13}C spectrum of *p*-acetamidobenzenesulfonyl azide **9**.

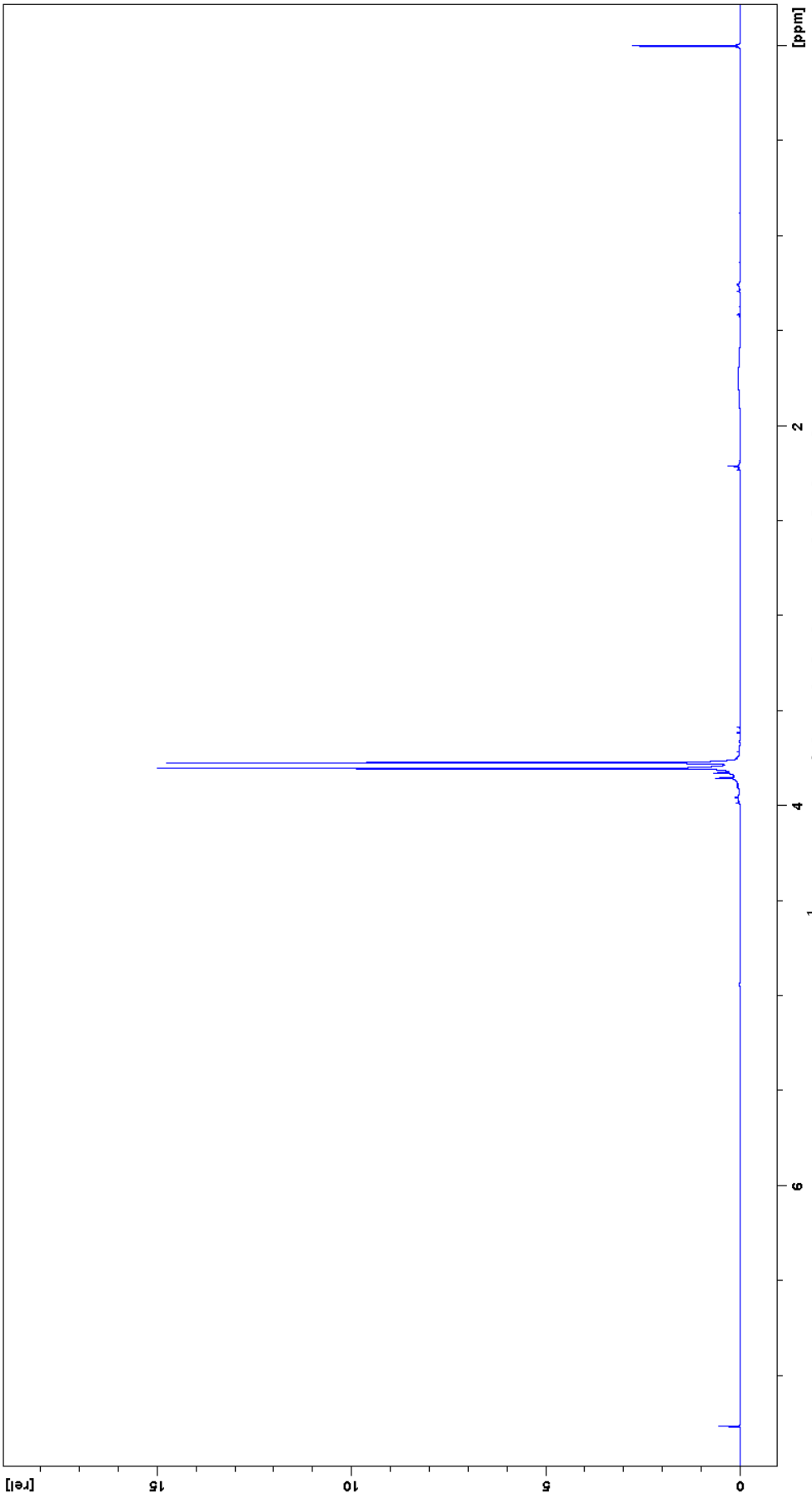

Figure 25: 400 MHz ^{1}H spectrum of dimethyl (diazomethyl)phosphonate **11**.

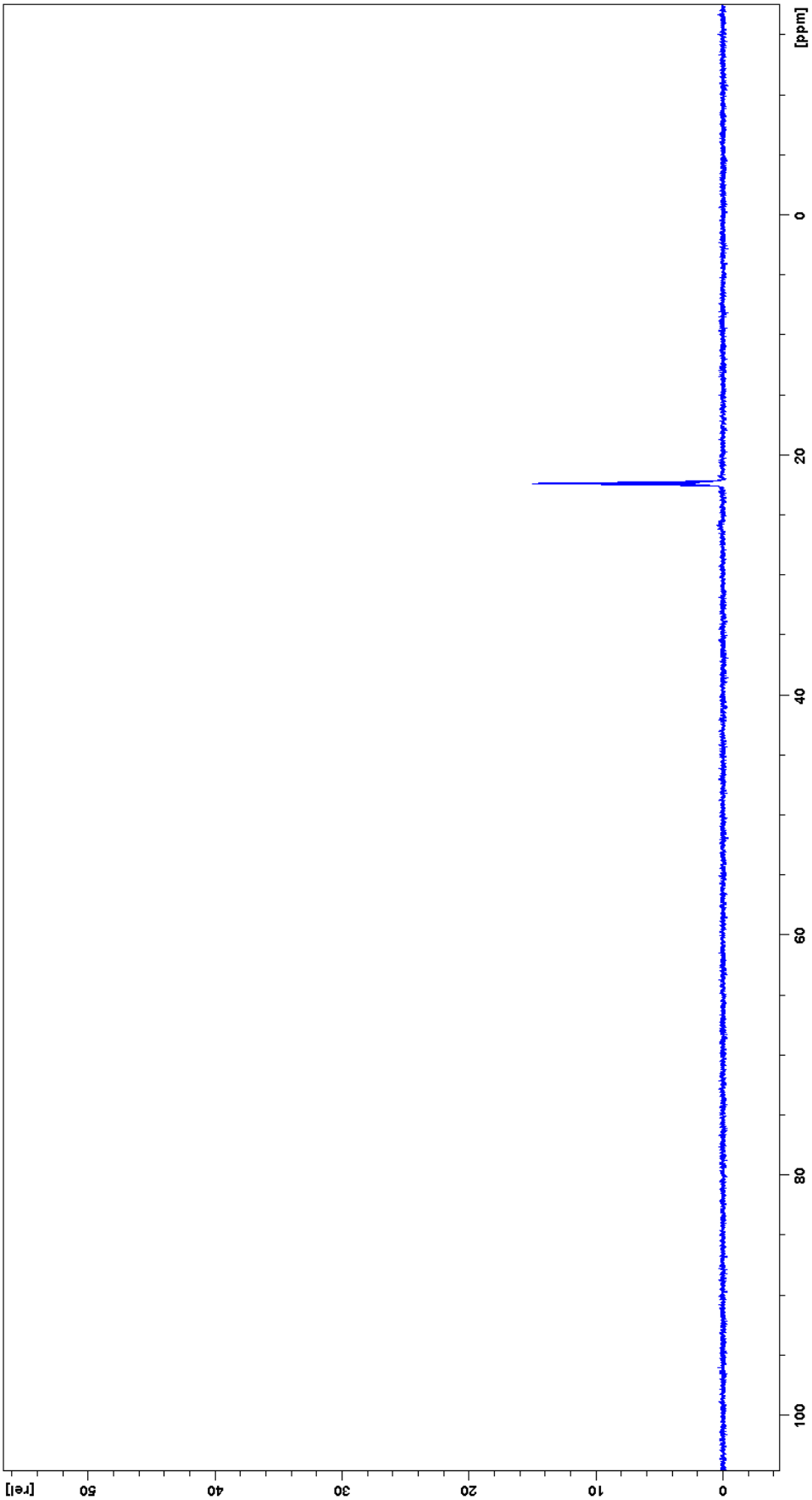

Figure 26: 161 MHz ^{31}P spectrum of dimethyl (diazomethyl) phosphonate **11**.

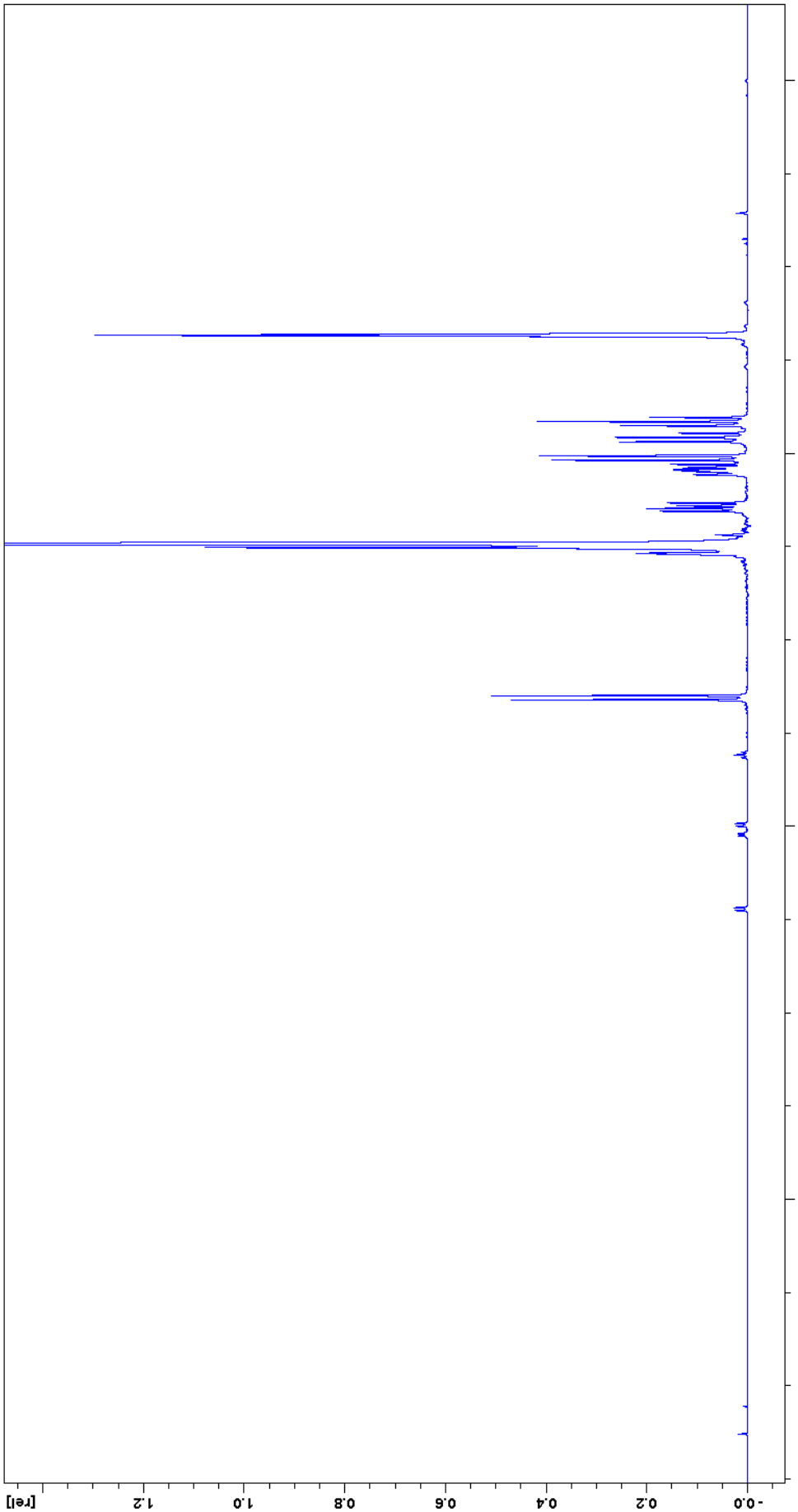

Figure 27: 400 MHz spectrum of deprotected glucosyl azide **13.**

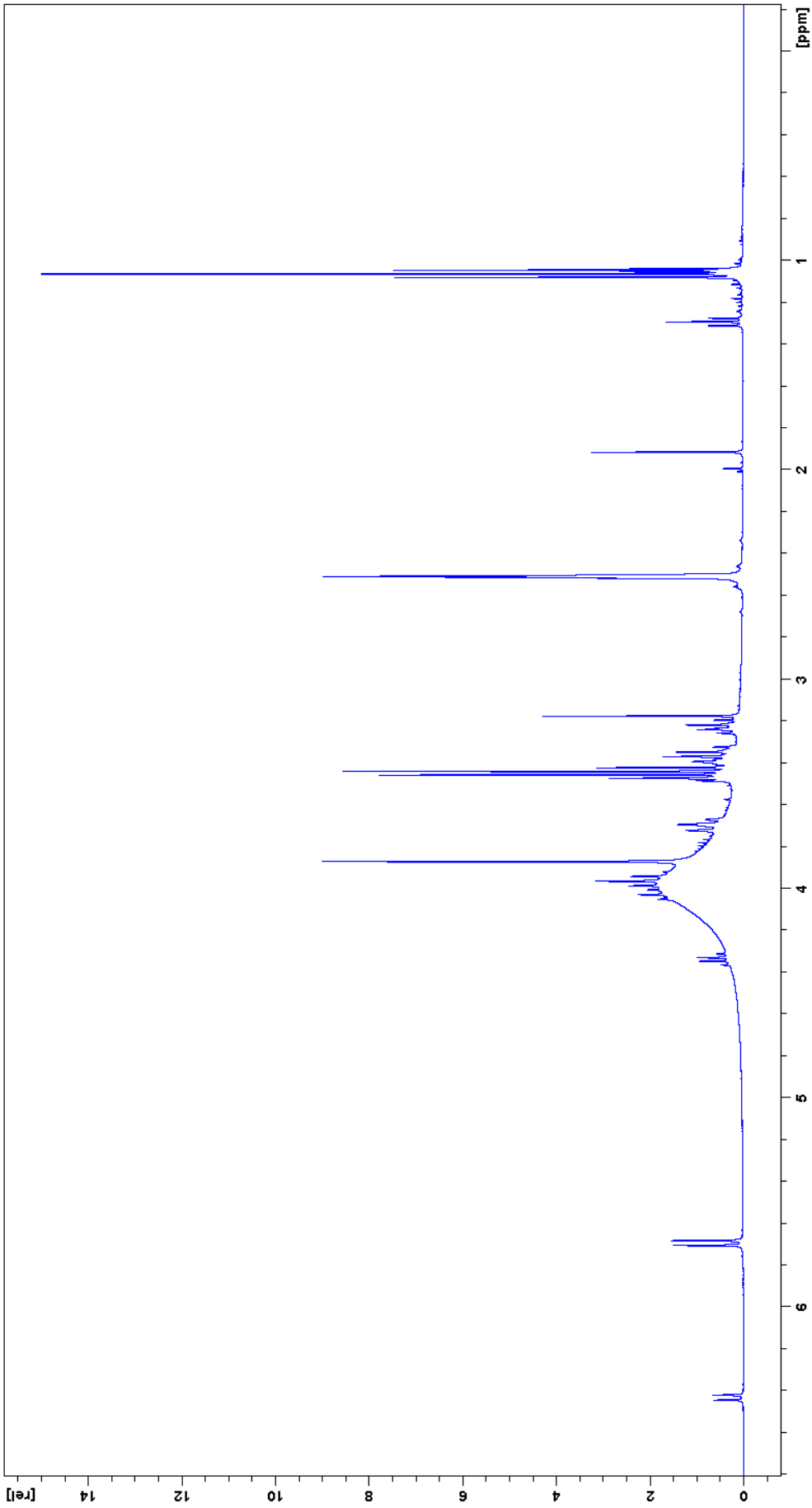

Figure 28: 400 MHz ^{1}H spectrum of deprotected glucosyl triazole **15**.

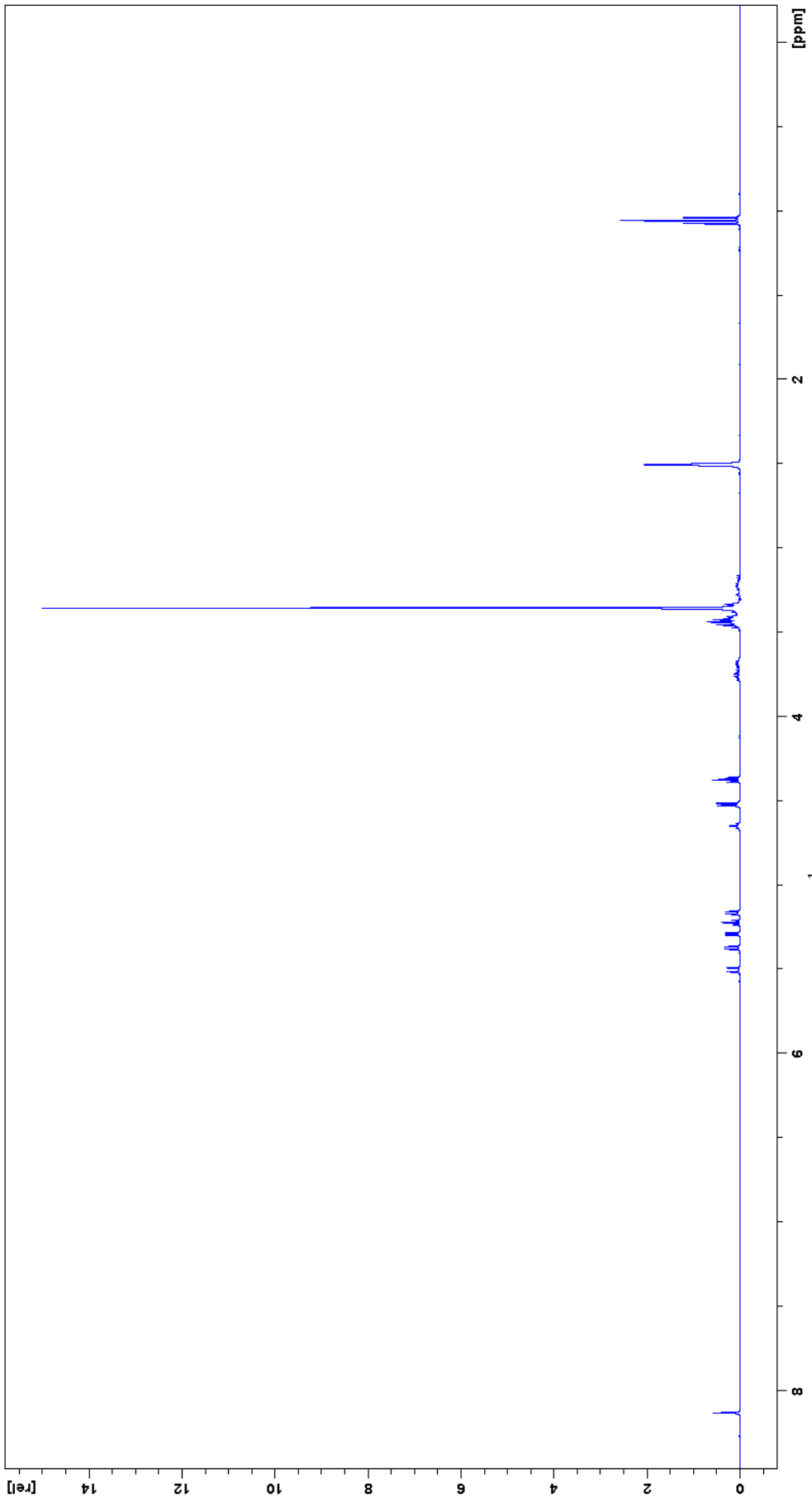

Figure 29: 400 MHz ^{1}H spectrum of deprotected glucosyl triazole **14**.

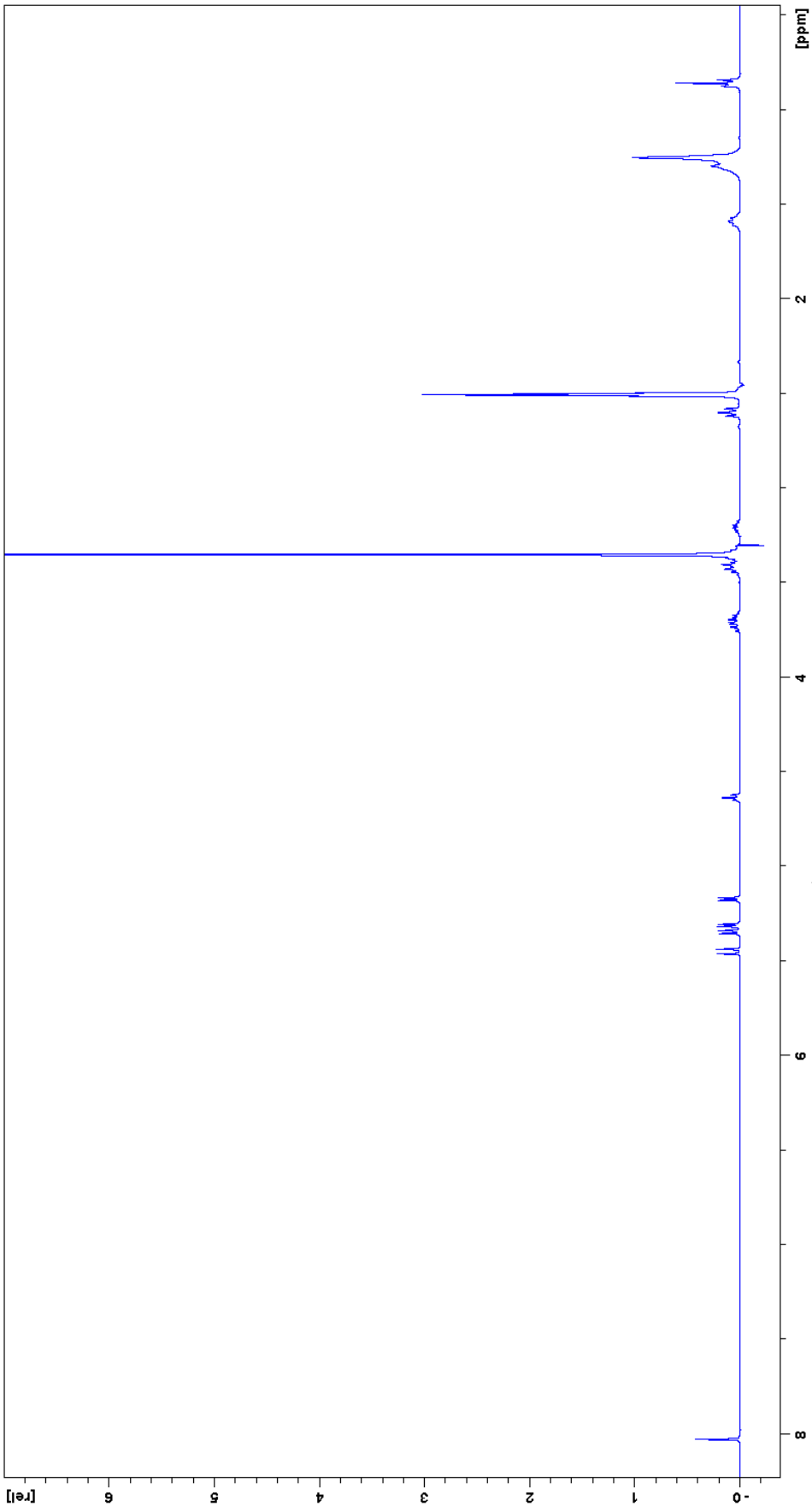

Figure 30: 400 MHz ^{1}H spectrum of deprotected glucosyl triazole **16.**

Appendix B

X-Ray Crystallography

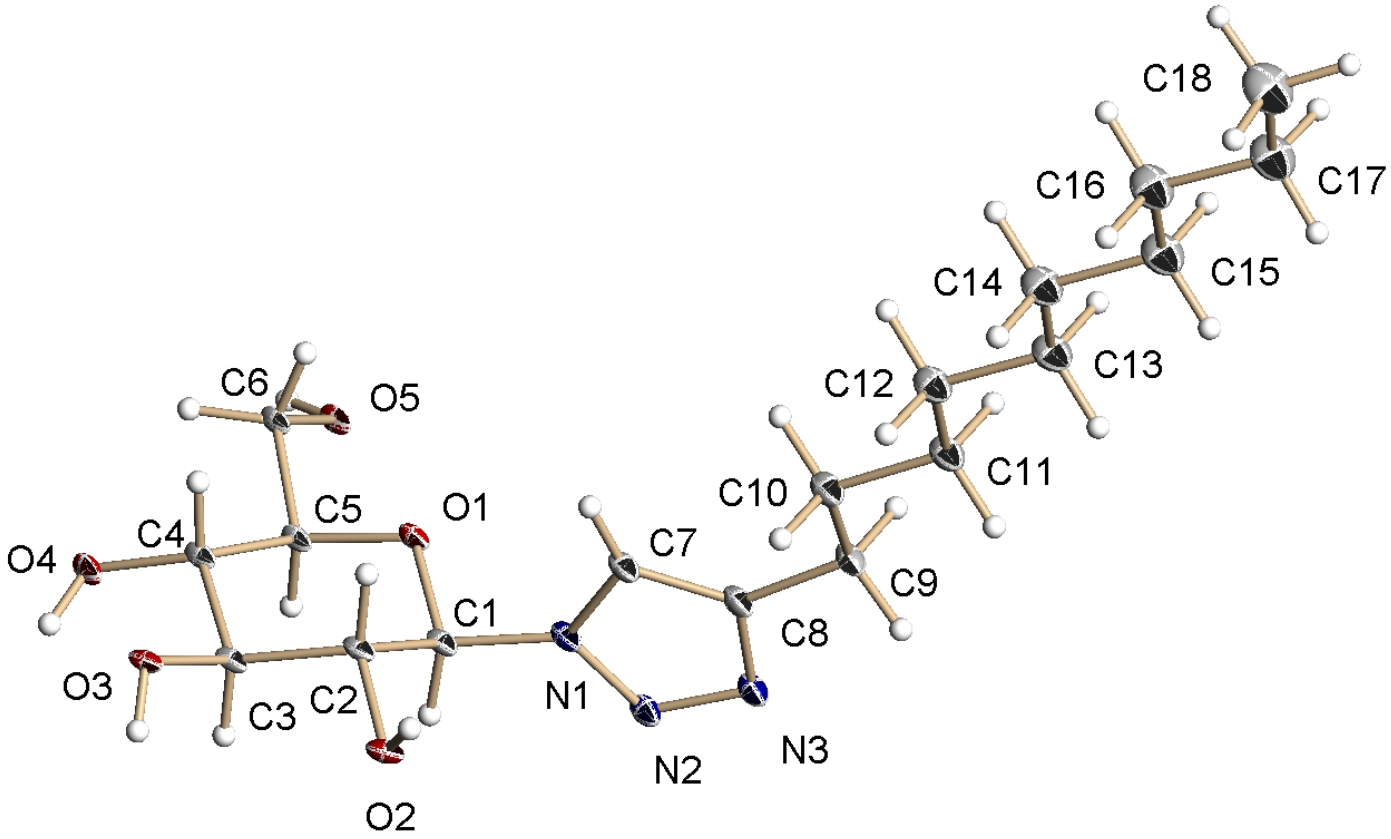

Figure 31: X-Ray crystal structure of glucosyl triazole **16**.

Table 1. Crystal data and structure refinement for 09mz041_0m:

Identification code: 09mz041_0m
Empirical formula: C18 H33 N3 O5
Formula weight: 371.47
Temperature: 100(2) K
Wavelength: 0.71073 Å
Crystal system: Monoclinic
Space group: C2
Unit cell dimensions:
a = 8.455(3) Å, α = 90°
b = 6.743(2) Å, β = 96.815(6)°
c = 34.019(12) Å, γ = 90°
Volume, *Z*: 1925.6(11) Å^3, 4
Density (calculated): 1.281 Mg/m^3
Absorption coefficient: 0.093 mm^{-1}
F(000): 808
Crystal size: 0.22 × 0.16 × 0.02 mm
Crystal shape, colour: plate, colourless
θ range for data collection: 1.81 to 26.37°
Limiting indices: -10 ≤ *h* ≤ 10, -8 ≤ *k* ≤ 8 -36 ≤ *l* ≤ 41
Reflections collected: 6174
Independent reflections: 2117 (*R*(int) = 0.0804)
Completeness to θ = 26.37°: 98.1 %
Absorption correction: multi-scan
Max. and min. transmission: 0.998 and 0.794
Refinement method: Full-matrix least-squares on F^2
Data / restraints / parameters: 2117 / 381 / 240
Goodness-of-fit on F^2: 1.169
Final *R* indices [$I>2\sigma(I)$]: R1 = 0.1205, wR2 = 0.2690
R indices (all data): R1 = 0.1450, wR2 = 0.2803
Largest diff. peak and hole: 0.596 and -0.627 e × Å^{-3}

Refinement of F^2 against ALL reflections. The weighted R-factor wR and goodness of fit are based on F^2, conventional R-factors R are based on *F*, with *F* set to zero for negative F^2. The threshold expression of $F^2 > 2\sigma(F^2)$ is used only for calculating R-factors

Comments:

The crystals suffered from low diffraction power and - despite long exposure times - no really good data set could be obtained. Besides the relatively high R values very anisotropic ADPs are the most prominent problem. No obvious reasons for these problems could be determined: The structure exhibits metric pseudosymmetry emulating a double volume F centered orthorhimbic cell as well as a same volume alternative C centered monoclinic cell with a the a and b axes exchanged. However, no twinning based on these similarities was found (max BASF values around 2% with no improvement of any quality indicators). The ADPs were thus vigourosly restrained using SIMU, DELU and ISOR commands with very low standard deviations (0.002, 0.002, and 0.01). No significant increase in R values was observed. No distance restraints were applied.

Treatment of hydrogen atoms:

All hydrogen atoms were placed in calculated positions and were refined with an isotropic displacement parameter 1.5 (methyl, hydroxyl) or 1.2 times (all others) that of the adjacent carbon atom.

Table 2. Atomic coordinates [× 10^4] and equivalent isotropic displacement parameters [Å^2 × 10^3] for 09mz041_0m. U(eq) is defined as one third of the trace of the orthogonalized U_{ij} tensor.

	x	y	z	U(eq)
C(1)	2111(11)	5385(15)	3532(3)	11(1)
C(2)	3048(11)	3476(15)	3523(3)	11(1)
C(3)	2885(11)	2364(15)	3909(3)	10(1)
C(4)	3503(11)	3579(15)	4262(3)	11(1)
C(5)	2703(11)	5671(15)	4239(3)	10(1)
C(6)	3528(10)	7022(15)	4563(3)	11(1)

C(7)	3357(11)	7065(16)	2963(3)	14(1)
C(8)	2681(11)	8072(15)	2649(3)	14(1)
C(9)	3318(11)	9170(15)	2313(3)	14(1)
C(10)	5004(11)	8507(17)	2237(3)	16(1)
C(11)	5524(12)	9664(17)	1882(3)	17(1)
C(12)	7176(12)	9084(17)	1780(3)	19(1)
C(13)	7641(12)	10220(18)	1426(3)	20(1)
C(14)	9285(12)	9645(19)	1306(3)	22(1)
C(15)	9729(12)	10823(19)	953(3)	24(1)
C(16)	11380(13)	10236(19)	833(3)	26(1)
C(17)	11802(13)	11390(20)	478(3)	27(1)
C(18)	13446(14)	10910(20)	350(4)	31(2)
N(1)	2128(9)	6537(13)	3174(3)	13(1)
N(2)	731(9)	7250(14)	2991(2)	13(1)
N(3)	1018(9)	8257(13)	2674(2)	14(1)
O(1)	2806(8)	6563(10)	3861(2)	11(1)
O(2)	2429(7)	2250(11)	3193(2)	14(1)
O(3)	3819(7)	545(10)	3930(2)	10(1)
O(4)	3213(8)	2682(10)	4625(2)	14(1)
O(5)	2543(8)	8680(10)	4634(2)	12(1)

All esds (except the esd in the dihedral angle between two l.s. planes) are estimated using the full covariance matrix. The cell esds are taken into account individually in the estimation of esds in distances, angles and torsion angles; correlations between esds in cell parameters are only used when they are defined by crystal symmetry. An approximate (isotropic) treatment of cell esds is used for estimating esds involving l.s. planes.

Table 3. Bond lengths [Å] and angles [deg] for 09mz041_0m.

C(1)-O(1)	1.440(12)	C(10)-C(11)	1.546(14)
C(1)-N(1)	1.447(13)	C(10)-H(10A)	0.9900
C(1)-C(2)	1.514(13)	C(10)-H(10B)	0.9900
C(1)-H(1)	1.0000	C(11)-C(12)	1.529(13)
C(2)-O(2)	1.440(12)	C(11)-H(11A)	0.9900
C(2)-C(3)	1.534(13)	C(11)-H(11B)	0.9900
C(2)-H(2)	1.0000	C(12)-C(13)	1.518(14)
C(3)-O(3)	1.456(11)	C(12)-H(12A)	0.9900
C(3)-C(4)	1.494(14)	C(12)-H(12B)	0.9900
C(3)-H(3)	1.0000	C(13)-C(14)	1.544(13)
C(4)-O(4)	1.422(12)	C(13)-H(13A)	0.9900
C(4)-C(5)	1.563(13)	C(13)-H(13B)	0.9900
C(4)-H(4)	1.0000	C(14)-C(15)	1.523(15)
C(5)-O(1)	1.429(12)	C(14)-H(14A)	0.9900
C(5)-C(6)	1.534(13)	C(14)-H(14B)	0.9900
C(5)-H(5)	1.0000	C(15)-C(16)	1.551(14)
C(6)-O(5)	1.432(11)	C(15)-H(15A)	0.9900
C(6)-H(6A)	0.9900	C(15)-H(15B)	0.9900
C(6)-H(6B)	0.9900	C(16)-C(17)	1.515(16)
C(7)-C(8)	1.337(14)	C(16)-H(16A)	0.9900
C(7)-N(1)	1.378(12)	C(16)-H(16B)	0.9900
C(7)-H(7)	0.9500	C(17)-C(18)	1.539(15)
C(8)-N(3)	1.424(12)	C(17)-H(17A)	0.9900
C(8)-C(9)	1.512(13)	C(17)-H(17B)	0.9900
C(9)-C(10)	1.545(12)	C(18)-H(18A)	0.9800
C(9)-H(9A)	0.9900	C(18)-H(18B)	0.9800
C(9)-H(9B)	0.9900	C(18)-H(18C)	0.9800

N(1)-N(2)	1.355(11)	C(3)-C(4)-C(5)	110.3(8)
N(2)-N(3)	1.322(11)	O(4)-C(4)-H(4)	108.6
O(2)-H(2A)	0.8400	C(3)-C(4)-H(4)	108.6
O(3)-H(3A)	0.8400	C(5)-C(4)-H(4)	108.6
O(4)-H(4A)	0.8400	O(1)-C(5)-C(6)	109.0(8)
O(5)-H(5A)	0.8400	O(1)-C(5)-C(4)	110.7(7)
		C(6)-C(5)-C(4)	110.0(8)
O(1)-C(1)-N(1)	108.3(8)	O(1)-C(5)-H(5)	109.1
O(1)-C(1)-C(2)	108.7(7)	C(6)-C(5)-H(5)	109.1
N(1)-C(1)-C(2)	112.4(8)	C(4)-C(5)-H(5)	109.1
O(1)-C(1)-H(1)	109.1	O(5)-C(6)-C(5)	111.1(7)
N(1)-C(1)-H(1)	109.1	O(5)-C(6)-H(6A)	109.4
C(2)-C(1)-H(1)	109.1	C(5)-C(6)-H(6A)	109.4
O(2)-C(2)-C(1)	111.2(8)	O(5)-C(6)-H(6B)	109.4
O(2)-C(2)-C(3)	109.0(8)	C(5)-C(6)-H(6B)	109.4
C(1)-C(2)-C(3)	107.2(7)	H(6A)-C(6)-H(6B)	108.0
O(2)-C(2)-H(2)	109.8	C(8)-C(7)-N(1)	105.7(8)
C(1)-C(2)-H(2)	109.8	C(8)-C(7)-H(7)	127.1
C(3)-C(2)-H(2)	109.8	N(1)-C(7)-H(7)	127.1
O(3)-C(3)-C(4)	106.7(8)	C(7)-C(8)-N(3)	109.1(8)
O(3)-C(3)-C(2)	110.4(7)	C(7)-C(8)-C(9)	134.1(9)
C(4)-C(3)-C(2)	111.2(8)	N(3)-C(8)-C(9)	116.4(8)
O(3)-C(3)-H(3)	109.5	C(8)-C(9)-C(10)	113.8(8)
C(4)-C(3)-H(3)	109.5	C(8)-C(9)-H(9A)	108.8
C(2)-C(3)-H(3)	109.5	C(10)-C(9)-H(9A)	108.8
O(4)-C(4)-C(3)	112.5(8)	C(8)-C(9)-H(9B)	108.8
O(4)-C(4)-C(5)	108.0(7)	C(10)-C(9)-H(9B)	108.8

H(9A)-C(9)-H(9B)	107.7	C(13)-C(14)-H(14A)	109.0
C(9)-C(10)-C(11)	109.8(8)	C(15)-C(14)-H(14B)	109.0
C(9)-C(10)-H(10A)	109.7	C(13)-C(14)-H(14B)	109.0
C(11)-C(10)-H(10A)	109.7	H(14A)-C(14)-H(14B)	107.8
C(9)-C(10)-H(10B)	109.7	C(14)-C(15)-C(16)	112.8(10)
C(11)-C(10)-H(10B)	109.7	C(14)-C(15)-H(15A)	109.0
H(10A)-C(10)-H(10B)	108.2	C(16)-C(15)-H(15A)	109.0
C(12)-C(11)-C(10)	113.6(9)	C(14)-C(15)-H(15B)	109.0
C(12)-C(11)-H(11A)	108.9	C(16)-C(15)-H(15B)	109.0
C(10)-C(11)-H(11A)	108.9	H(15A)-C(15)-H(15B)	107.8
C(12)-C(11)-H(11B)	108.9	C(17)-C(16)-C(15)	112.5(10)
C(10)-C(11)-H(11B)	108.9	C(17)-C(16)-H(16A)	109.1
H(11A)-C(11)-H(11B)	107.7	C(15)-C(16)-H(16A)	109.1
C(13)-C(12)-C(11)	112.3(9)	C(17)-C(16)-H(16B)	109.1
C(13)-C(12)-H(12A)	109.1	C(15)-C(16)-H(16B)	109.1
C(11)-C(12)-H(12A)	109.1	H(16A)-C(16)-H(16B)	107.8
C(13)-C(12)-H(12B)	109.1	C(16)-C(17)-C(18)	115.1(11)
C(11)-C(12)-H(12B)	109.1	C(16)-C(17)-H(17A)	108.5
H(12A)-C(12)-H(12B)	107.9	C(18)-C(17)-H(17A)	108.5
C(12)-C(13)-C(14)	114.2(9)	C(16)-C(17)-H(17B)	108.5
C(12)-C(13)-H(13A)	108.7	C(18)-C(17)-H(17B)	108.5
C(14)-C(13)-H(13A)	108.7	H(17A)-C(17)-H(17B)	107.5
C(12)-C(13)-H(13B)	108.7	C(17)-C(18)-H(18A)	109.5
C(14)-C(13)-H(13B)	108.7	C(17)-C(18)-H(18B)	109.5
H(13A)-C(13)-H(13B)	107.6	H(18A)-C(18)-H(18B)	109.5
C(15)-C(14)-C(13)	113.1(10)	C(17)-C(18)-H(18C)	109.5
C(15)-C(14)-H(14A)	109.0	H(18A)-C(18)-H(18C)	109.5

H(18B)-C(18)-H(18C)	109.5
N(2)-N(1)-C(7)	109.8(8)
N(2)-N(1)-C(1)	118.8(7)
C(7)-N(1)-C(1)	131.3(8)
N(3)-N(2)-N(1)	108.9(7)
N(2)-N(3)-C(8)	106.4(8)
C(5)-O(1)-C(1)	113.7(7)
C(2)-O(2)-H(2A)	109.5
C(3)-O(3)-H(3A)	109.5
C(4)-O(4)-H(4A)	109.5
C(6)-O(5)-H(5A)	109.5

Table 4. Anisotropic displacement parameters [$Å^2 \times 10^3$] for 09mz041_0m. The anisotropic displacement factor exponent takes the form: $-2\pi^2 [(h\ a^*)^2 U11 + ... + 2\ h\ k\ a^*\ b^*\ U12]$

	U11	U22	U33	U23	U13	U12
C(1)	9(1)	8(1)	17(1)	1(1)	4(1)	-1(1)
C(2)	8(2)	8(1)	17(1)	-1(1)	4(1)	-1(1)
C(3)	7(2)	6(1)	18(1)	-1(1)	4(1)	0(1)
C(4)	9(2)	6(1)	17(1)	-1(1)	4(1)	1(1)
C(5)	9(2)	5(1)	17(1)	0(1)	3(1)	0(1)
C(6)	10(2)	5(2)	18(2)	0(2)	3(2)	1(2)
C(7)	11(2)	11(2)	19(2)	3(2)	4(1)	-1(2)
C(8)	12(2)	10(2)	20(2)	3(2)	4(1)	-1(2)
C(9)	13(2)	10(2)	21(2)	4(2)	5(1)	0(2)
C(10)	14(2)	13(2)	22(2)	3(2)	5(2)	1(2)
C(11)	15(2)	15(2)	22(2)	2(2)	6(2)	0(2)
C(12)	16(2)	18(2)	23(2)	1(2)	6(2)	-1(2)
C(13)	17(2)	21(2)	23(2)	1(2)	7(2)	-2(2)
C(14)	19(2)	24(2)	25(2)	1(2)	8(2)	-2(2)
C(15)	21(2)	26(2)	26(2)	2(2)	9(2)	-2(2)
C(16)	23(2)	28(3)	27(2)	2(2)	10(2)	-1(2)
C(17)	25(2)	30(3)	29(3)	2(2)	11(2)	-2(2)
C(18)	29(3)	34(4)	33(4)	0(3)	16(3)	-1(3)
N(1)	10(2)	10(2)	18(1)	2(1)	4(1)	-1(1)
N(2)	11(2)	10(2)	19(2)	2(2)	4(1)	1(2)
N(3)	12(2)	10(2)	20(2)	3(2)	5(1)	1(2)
O(1)	10(2)	7(1)	18(1)	0(1)	4(1)	-1(1)

O(2)	11(2)	13(2)	19(2)	-3(2)	3(2)	-5(2)
O(3)	4(2)	6(2)	21(3)	-2(2)	2(2)	1(2)
O(4)	16(3)	6(2)	18(2)	1(2)	2(2)	0(2)
O(5)	11(2)	4(2)	21(3)	-1(2)	3(2)	2(2)

Table 5. Hydrogen coordinates ($\times 10^4$) and isotropic displacement parameters ($Å^2 \times 10^3$) for 09mz041_0m.

	x	y	z	U(eq)
H(1)	984	5064	3570	14
H(2)	4195	3783	3505	13
H(3)	1739	2034	3923	12
H(4)	4678	3751	4263	13
H(5)	1555	5527	4278	13
H(6A)	3772	6253	4811	13
H(6B)	4547	7506	4482	13
H(7)	4456	6773	3028	16
H(9A)	3342	10607	2374	17
H(9B)	2579	8970	2068	17
H(10A)	5003	7067	2180	19
H(10B)	5768	8757	2476	19
H(11A)	4735	9431	1647	21
H(11B)	5520	11101	1942	21
H(12A)	7972	9341	2012	22
H(12B)	7189	7645	1722	22
H(13A)	7645	11656	1487	24
H(13B)	6822	9991	1197	24
H(14A)	10107	9864	1534	26
H(14B)	9281	8215	1240	26
H(15A)	9736	12254	1018	29
H(15B)	8907	10606	724	29
H(16A)	12205	10476	1060	31

H(16B)	11380	8800	772	31
H(17A)	11765	12821	538	33
H(17B)	10979	11123	252	33
H(18A)	14265	11048	577	47
H(18B)	13671	11821	140	47
H(18C)	13448	9540	251	47
H(2A)	3114	2143	3035	22
H(3A)	3273	-372	3815	15
H(4A)	2967	1486	4585	20
H(5A)	2468	8766	4877	18

Table 6. Torsion angles [deg] for 09mz041_0m

O(1)-C(1)-C(2)-O(2)	-178.7(7)
N(1)-C(1)-C(2)-O(2)	-58.8(10)
O(1)-C(1)-C(2)-C(3)	62.3(9)
N(1)-C(1)-C(2)-C(3)	-177.9(8)
O(2)-C(2)-C(3)-O(3)	62.1(9)
C(1)-C(2)-C(3)-O(3)	-177.4(7)
O(2)-C(2)-C(3)-C(4)	-179.7(7)
C(1)-C(2)-C(3)-C(4)	-59.2(9)
O(3)-C(3)-C(4)-O(4)	-65.9(9)
C(2)-C(3)-C(4)-O(4)	173.7(7)
O(3)-C(3)-C(4)-C(5)	173.4(7)
C(2)-C(3)-C(4)-C(5)	53.0(9)
O(4)-C(4)-C(5)-O(1)	-173.8(7)
C(3)-C(4)-C(5)-O(1)	-50.5(9)
O(4)-C(4)-C(5)-C(6)	65.7(9)
C(3)-C(4)-C(5)-C(6)	-170.9(8)
O(1)-C(5)-C(6)-O(5)	77.2(9)
C(4)-C(5)-C(6)-O(5)	-161.3(7)
N(1)-C(7)-C(8)-N(3)	2.8(12)
N(1)-C(7)-C(8)-C(9)	175.6(11)
C(7)-C(8)-C(9)-C(10)	22.2(17)
N(3)-C(8)-C(9)-C(10)	-165.4(9)
C(8)-C(9)-C(10)-C(11)	178.2(9)
C(9)-C(10)-C(11)-C(12)	-179.2(9)
C(10)-C(11)-C(12)-C(13)	179.1(9)

C(11)-C(12)-C(13)-C(14)	-178.6(10)
C(12)-C(13)-C(14)-C(15)	-179.4(10)
C(13)-C(14)-C(15)-C(16)	-179.9(10)
C(14)-C(15)-C(16)-C(17)	179.0(10)
C(15)-C(16)-C(17)-C(18)	178.7(11)
C(8)-C(7)-N(1)-N(2)	-1.0(12)
C(8)-C(7)-N(1)-C(1)	177.8(10)
O(1)-C(1)-N(1)-N(2)	-108.4(9)
C(2)-C(1)-N(1)-N(2)	131.5(9)
O(1)-C(1)-N(1)-C(7)	73.0(13)
C(2)-C(1)-N(1)-C(7)	-47.1(14)
C(7)-N(1)-N(2)-N(3)	-1.4(11)
C(1)-N(1)-N(2)-N(3)	179.7(9)
N(1)-N(2)-N(3)-C(8)	3.0(11)
C(7)-C(8)-N(3)-N(2)	-3.7(12)
C(9)-C(8)-N(3)-N(2)	-177.9(9)
C(6)-C(5)-O(1)-C(1)	178.1(7)
C(4)-C(5)-O(1)-C(1)	57.0(9)
N(1)-C(1)-O(1)-C(5)	173.5(7)
C(2)-C(1)-O(1)-C(5)	-64.1(9)

Table 7. Hydrogen bonds for 09mz041_0m [Å and deg].

D-H...A	d(D-H)	d(H...A)	d(D...A)	<(DHA)
O(5)-H(5A)...O(4)#1	0.84	1.99	2.758(9)	151.2
O(4)-H(4A)...O(5)#2	0.84	1.94	2.758(10)	165.7
O(3)-H(3A)...O(1)#2	0.84	2.11	2.819(10)	141.5
O(2)-H(2A)...N(2)#3	0.84	2.24	2.954(10)	143.5

Symmetry transformations used to generate equivalent atoms:

#1 -x+1/2,y+1/2,-z+1 #2 x,y-1,z #3 x+1/2,y-1/2,z